arXiv:1601.01379v1 [cs.IT] 7 Jan 2016

User-Centric Interference Nulling in Downlink Multi-Antenna Heterogeneous Networks

Ying Cui, Yueping Wu, Dongdong Jiang, Bruno Clerckx

Abstract

Heterogeneous networks (HetNets) are subject to strong interference due to spectrum reuse. This affects the signal-to-interference ratio (SIR) of each user, and hence is one of the limiting factors of network performance. However, in previous works, interference management approaches in HetNets are mainly based on signal or interference level, and thus cannot effectively improve network performance. In this paper, we propose a user-centric interference nulling (IN) scheme in downlink large-scale HetNets to improve network performance by improving each user's SIR. This scheme has three design parameters: the maximum degree of freedom for IN (i.e., maximum IN DoF), and the IN thresholds for macro and pico users, respectively. Using tools from stochastic geometry, we first obtain a tractable expression of the coverage (equivalently outage) probability. Then, we obtain the asymptotic expressions of the outage and coverage probabilities in the low and high SIR threshold regimes, respectively. The asymptotic expressions indicate that the maximum IN DoF and the IN thresholds affect the asymptotic outage (coverage) probability in dramatically different ways. Moreover, we characterize the optimal maximum IN DoF which optimizes the asymptotic outage (coverage) probability. The optimization results reveal that the IN scheme can linearly improve the performance in the low SIR threshold regime, but cannot improve the performance in the high SIR threshold regime. Finally, numerical results show that the user-centric IN scheme can achieve good performance gains over existing schemes.

Index Terms

Heterogeneous networks, multiple antennas, inter-tier interference coordination, stochastic geometry, optimization.

Y. Cui and D. Jiang are with the Department of Electronic Engineering, Shanghai Jiao Tong University, China. Y. Wu and B. Clerckx are with Department of Electrical and Electronic Engineering, Imperial College London, United Kingdom. B. Clerckx is also with School of Electrical Engineering, Korea University, Korea. This work was presented in part in IEEE ISIT 2015.

I. Introduction

The modern wireless networks have seen a significant growth of high data rate applications. The conventional cellular solution, which comprises of high power base stations (BSs), cannot scale with the increasing data rate demand. One solution is the deployment of low power small cell BSs overlaid with conventional large power macro-BSs, so called heterogeneous networks (HetNets) [1, 2]. HetNets are capable of aggressively reusing existing spectrum assets to support high data rate applications. However, spectrum reuse in HetNets causes strong interference. This affects the signal-to-interference ratio (SIR) of each user, and hence is one of the limiting factors of network performance. Interference management techniques are thus desirable in HetNets [3]. One such technique is interference cooperation. For example, in [4–6], different interference cooperation strategies are considered and their performances are analyzed for large-scale HetNets under random models using tools from stochastic geometry [7, 8]. Specifically, [4] proposes an interference cooperation strategy among a fixed number of BSs from different tiers of a HetNet which jointly provide the strongest average receive power for the typical user. Reference [5] proposes an interference cooperation strategy among BSs from different tiers of a HetNet which provide long-term average received powers for the typical user above thresholds of different tiers. Reference [6] proposes an interference cooperation strategy among BSs from different tiers of a HetNet where the typical user is either served by its nearest (single) BS or nearest marco and pico BSs jointly. However, in [4–6], the cooperation clusters are formed to favor the typical user only, and hence, the analytical performance of the typical user is better than the actual network performance (of all the users). In addition, [4–6] only consider single-antenna BSs. Orthogonalizing the time or frequency resource allocated to macro cells and small cells can also mitigate interference in HetNets. One such technique is almost blank subframes (ABS) in 3GPP LTE [9]. In ABS, the time or frequency resource is partitioned, whereby offloaded users and the other users are served using different portions of the resource. The performance of ABS in large-scale HetNets with offloading is analyzed in [9] using tools from stochastic geometry. Note that ABS mitigates the interference of offloaded users, and [9] only considers single-antenna BSs.

Deploying multiple antennas at each BS in HetNets can further improve network performance. With multiple antennas, besides boosting the desired signal to each user, more effective inter-

ference management techniques can be implemented. For example, interference coordination strategies are proposed and analyzed in [10–14]. In [10–12], the authors consider a HetNet with a single multi-antenna macro-BS and multiple small-BSs, where the multiple antennas at the macro-BS are used for serving its scheduled users as well as mitigating the interference to the small cell users using different interference coordination schemes. These schemes are analyzed and shown to improve the performance of the HetNet. However, since only one macro-BS is considered, the analytical results obtained in [10–12] cannot reflect the macro-tier interference, and thus may not offer accurate insights for practical HetNets. Reference [14] proposes an interference nulling scheme where some degree of freedom at each macro-BS can be used for avoiding its interference to some of its offloaded users. The amount of degree of freedom for interference nulling is an adjustable parameter and is optimized to improve the network performance. However, the interference nulling scheme proposed in [14] only improves the performance of offloaded users, and hence may not effectively improve the overall network performance. In [13], a fixed number of BSs which provide the strongest average received power for the typical user form a cluster, and adopt an interference coordination scheme in a large-scale multi-antenna HetNet, where the BSs in each cluster mitigate interference to users in this cluster. Bounds of the coverage probability are derived based on the assumption that the BSs in each cluster are the strongest BSs of all the users in this cluster.

The investigation of interference management techniques in large-scale single-tier multi-antenna cellular networks is less involved than that in large-scale multi-antenna HetNets, and hence has been more extensively conducted (see [15, 16] [17] [18] and the references therein). In [17] [15] [18], all the BSs are grouped into disjoint clusters. Coordination [17] [15] and cooperation [18] are performed among the BSs within each cluster to mitigate intra-cluster interference. Specifically, [17] and [15] design disjoint BS clustering from a transmitter's point of view and fail to consider each user's interference situation. The dynamic clustering proposed in [18] considers all the users' signal and interference situations to optimize the network performance. However, it requires centralized control and may not be suitable for large networks. Recently, a novel distributed user-centric IN scheme, which takes account of each user's desired signal strength and interference level, is proposed and analyzed for single-tier multi-antenna cellular networks in [16]. However, in [16], the maximum degree of freedom for IN (i.e., maximum IN DoF) at each BS is not adjustable, and thus cannot properly exploit limited resource in single-

tier cellular networks. Moreover, directly applying the scheme in [16] to HetNets cannot fully exploit different properties of macro and pico users in HetNets.

In this paper, we consider the downlink large-scale two-tier multi-antenna HetNets and propose a user-centric IN scheme to improve network performance by improving each user's SIR. In this scheme, each scheduled macro (pico) user first sends an IN request to a macro-BS[1] if the power ratio of its desired signal and the interference from the macro-BS, referred to as the signal-to-individual-interference ratio (SIIR), is below an IN threshold for macro (pico) users. Then, each macro-BS utilizes zero-forcing beamforming (ZFBF) precoder to avoid interference to at most U scheduled users which send IN requests to it as well as boost the desired signal to its scheduled user. This scheme has three design parameters: the maximum IN DoF U, and the IN thresholds for macro and pico users, respectively. In general, the performance analysis and optimization of interference management techniques in large-scale multi-antenna HetNets are very challenging, mainly due to i) the statistical dependence among macro-BSs and pico-BSs [10], ii) the complex distribution of desired signal using multi-antenna communication schemes, and iii) the complicated interference distribution caused by interference management techniques (e.g., beamforming). Our main contributions are summarized below. The analytical and numerical results obtained in this paper provide valuable design insights for practical HetNets.

- We obtain a tractable expression of the coverage (equivalently outage) probability, by adopting appropriate approximations and utilizing tools from stochastic geometry.
- We obtain the asymptotic expressions of the outage and coverage probabilities in the low and high SIR threshold regimes, respectively, using series expansions of special functions. The asymptotic expressions indicate that the maximum IN DoF and the IN thresholds affect the asymptotic outage (coverage) probability in dramatically different ways.
- We consider the optimizations of the maximum IN DoF for given IN thresholds in the two asymptotic regimes, which are challenging integer programming problems with very complicated objective functions. By exploiting the structure of each objective function, we characterize the optimal maximum IN DoF. The optimization results reveal that the IN

[1]Note that, compared to a pico-BS, a macro-BS usually causes stronger interference due to larger transmit power, and has a better capability of performing spatial cancellation due to a larger number of transmit antennas. Thus, it is more advisable to perform IN at macro-BSs.

scheme can linearly improve the performance in the low SIR threshold regime, but cannot improve the performance in the high SIR threshold regime.

- We show that the IN scheme can achieve good performance gains over existing schemes, using numerical results.

II. Network Model

We consider a two-tier HetNet where a macro-cell tier is overlaid with a pico-cell tier, as shown in Fig. 1. The locations of the macro-BSs and the pico-BSs are spatially distributed as two independent homogeneous Poisson point processes (PPPs) Φ_1 and Φ_2 with densities λ_1 and λ_2, respectively. The locations of the users are also distributed as an independent homogeneous PPP Φ_u with density λ_u. Without loss of generality, denote the macro-cell tier as the 1st tier and the pico-cell tier as the 2nd tier. We focus on the downlink scenario. Each macro-BS has N_1 antennas with total transmission power P_1, each pico-BS has N_2 antennas with total transmission power P_2, and each user has a single antenna. Assume $N_1 > N_2$. We consider both large-scale fading and small-scale fading. Specifically, due to large-scale fading, transmitted signals from the jth tier with distance r are attenuated by a factor $\frac{1}{r^{\alpha_j}}$, where $\alpha_j > 2$ is the path loss exponent of the jth tier and $j = 1, 2$. For small-scale fading, we assume Rayleigh fading channels.

A. User Association

We assume open access [4]. User i (denoted as u_i) is associated with the BS which provides the maximum *long-term average* received power among all the macro-BSs and pico-BSs. This associated BS is called the *serving BS* of user i. Note that within each tier, the nearest BS to user i provides the strongest long-term average received power in this tier. User i is thus associated with (the nearest BS in) the j_i^*th tier, if[2] $j_i^* = \arg\max_{j\in\{1,2\}} P_j Z_{i,j}^{-\alpha_j}$, where $Z_{i,j}$ is the distance between user i and its nearest BS in the jth tier. We refer to the users associated with the macro-cell tier as the *macro-users*, denoted as $\mathcal{U}_1 \triangleq \left\{u_i | P_1 Z_{i,1}^{-\alpha_1} \geq P_2 Z_{i,2}^{-\alpha_2}\right\}$, and the users associated with the pico-cell tier as the *pico-users*, denoted as $\mathcal{U}_2 \triangleq \left\{u_i | P_2 Z_{i,2}^{-\alpha_2} > P_1 Z_{i,1}^{-\alpha_1}\right\}$. All the users can be partitioned into two disjoint user sets: $\mathcal{U}_1$ and $\mathcal{U}_2$. After the user association, each BS

[2]In the user association procedure, the first antenna is normally used to transmit signal (using the total transmission power of each BS) for received power determination according to LTE standards.

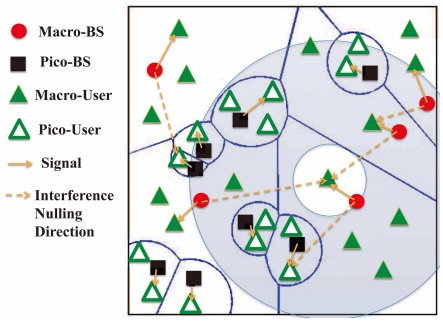

Fig. 1. System Model ($U = 1$).

schedules its associated users according to TDMA, i.e., scheduling one user in each time slot. Hence, there is no intra-cell interference.

B. Performance Metric

In this paper, we study the performance of the typical user denoted as u_0, which is a scheduled user located at the origin [19]. Since HetNets are interference-limited, we ignore the thermal noise in the analysis of this paper. Note that the analytical results with thermal noise can be calculated in a similar way [20]. We investigate the *coverage probability* of u_0, which is defined as the probability that the SIR of u_0 is larger than a threshold [4], i.e.,

$$\mathcal{S}(\beta) \triangleq \Pr\left(\mathrm{SIR}_0 > \beta\right) \tag{1}$$

where β is the SIR threshold.

III. User-centric Interference Nulling Scheme

In this section, we first elaborate on a user-centric IN scheme. Then, we obtain some distributions related to this scheme.

A. Scheme Description

First, we refer to an interfering macro-BS which causes the SIIR at a scheduled user i in the jth tier ($u_i \in \mathcal{U}_j$) below threshold $T_j \geq 1$ as a *potential IN macro-BS* of u_i, where $j = 1, 2$. We refer to T_j as the *IN threshold* for the jth tier. Mathematically, interfering macro-BS ℓ is a potential IN macro-BS of scheduled user $u_i \in \mathcal{U}_j$ if $\frac{P_j Z_{i,j}^{-\alpha_j}}{P_1 D_{1,\ell i}^{-\alpha_1}} < T_j$, where $D_{1,\ell i}$ is the distance

from macro-BS ℓ to u_i. Note that T_1 and T_2 are two design parameters of the IN scheme. In each time slot, each scheduled user sends IN requests to all of its potential IN macro-BSs. We refer to the scheduled users which send IN requests to interfering macro-BS ℓ as the *potential IN users* of interfering macro-BS ℓ (in this time slot). We introduce another design parameter $U \in \{0, 1, \cdots, N_1 - 1\}$ of this IN scheme, referred to as the *maximum IN DoF*. Consider a particular time slot. Let K_ℓ denote the number of the potential IN users of interfering macro-BS ℓ.[3] Consider two cases in the following. i) If $K_\ell > 0$ and $U > 0$, macro-BS ℓ makes use of at most U DoF to perform IN to some of its potential IN users. In particular, if $0 < K_\ell \leq U$, macro-BS ℓ can perform IN to all of its K_ℓ potential IN users using K_ℓ DoF; if $K_\ell > U$, macro-BS ℓ randomly selects U out of its K_ℓ potential IN users according to the uniform distribution, and perform IN to the selected U users using U DoF. Hence, in this case, macro-BS ℓ performs IN to $u_{\text{IN},\ell} \triangleq \min(U, K_\ell)$ potential IN users (referred to as the *IN users* of macro-BS ℓ) using $u_{\text{IN},\ell}$ DoF (referred to as the *IN DoF* of macro-BS ℓ). ii) If $K_\ell = 0$ or $U = 0$, macro-BS ℓ does not perform IN. In this case, we let $u_{\text{IN},\ell} = 0$. In both cases, $N_1 - u_{\text{IN},\ell}$ DoF at macro-BS ℓ is used for boosting the desired signal to its scheduled user.

Now, we introduce the precoding vectors at macro-BSs in the IN scheme. Consider two cases in the following. i) If $K_\ell > 0$ and $U > 0$, macro-BS ℓ utilizes the low-complexity ZFBF precoder to serve its scheduled user and simultaneously perform IN to its $u_{\text{IN},\ell}$ IN users. Specifically, denote $\mathbf{H}_{1,\ell} = \left[\mathbf{h}_{1,\ell}\ \mathbf{g}_{1,\ell 1}\ \cdots\ \mathbf{g}_{1,\ell u_{\text{IN},\ell}}\right]^\dagger$, where[4] $\mathbf{h}_{1,\ell} \overset{d}{\sim} \mathcal{CN}_{N_1,1}(\mathbf{0}_{N_1\times 1}, \mathbf{I}_{N_1})$ denotes the channel vector between macro-BS ℓ and its scheduled user, and $\mathbf{g}_{1,\ell i} \overset{d}{\sim} \mathcal{CN}_{N_1,1}(\mathbf{0}_{N_1\times 1}, \mathbf{I}_{N_1})$ denotes the channel vector between macro-BS ℓ and its ith IN user $(i = 1, \ldots, u_{\text{IN},\ell})$. The ZFBF precoding matrix at macro-BS ℓ is designed to be $\mathbf{W}_{1,\ell} = \mathbf{H}_{1,\ell}^\dagger \left(\mathbf{H}_{1,\ell}\mathbf{H}_{1,\ell}^\dagger\right)^{-1}$ and the ZFBF vector at macro-BS ℓ is designed to be $\mathbf{f}_{1,\ell} = \frac{\mathbf{w}_{1,\ell}}{\|\mathbf{w}_{1,\ell}\|}$, where $\mathbf{w}_{1,\ell}$ is the first column of $\mathbf{W}_{1,\ell}$. ii) If $K_\ell = 0$ or $U = 0$, macro-BS ℓ uses the maximal ratio transmission (MRT) precoder to serve its scheduled user, which is a special case of the ZFBF precoder introduced for $K_\ell > 0$ and $U > 0$, and can be readily obtained from it by letting $u_{\text{IN},\ell} = 0$, i.e., $\mathbf{H}_{1,\ell} = \mathbf{h}_{1,\ell}^\dagger$. Next, we introduce the precoding vectors at pico-BSs. Each pico-BS utilizes the MRT precoder to serve its scheduled user. Specifically, the beamforming vector at pico-BS ℓ is $\mathbf{f}_{2,\ell} = \frac{\mathbf{h}_{2,\ell}}{\left\|\mathbf{h}_{2,\ell}\right\|}$, where $\mathbf{h}_{2,\ell} \overset{d}{\sim} \mathcal{CN}_{N_2,1}(\mathbf{0}_{N_2\times 1}, \mathbf{I}_{N_2})$ denotes

[3]Note that $T_1 = T_2 = 1$ implies $K_\ell = 0$.

[4]The notation $X \overset{d}{\sim} Y$ means that X *is distributed as* Y.

the channel vector between pico-BS ℓ and its scheduled user. Note that the simple beamforming scheme (without interference management) can be included in the IN scheme as a special case by letting $T_1 = T_2 = 1$ and/or $U = 0$.[5]

Let $\mathbf{h}_{j,00}$ denote the channel vector between $u_0 \in \mathcal{U}_j$ and its serving BS $B_{j,0}$, $D_{j,\ell 0}$ denote the distance between u_0 and BS ℓ in the jth tier, Y_j denote the distance between u_0 and $B_{j,0}$, and $\mathbf{f}_{j,0}$ denote the beamforming vector at $B_{j,0}$, with $\left|\mathbf{h}_{j,00}^{\dagger}\mathbf{f}_{j,0}\right|^2 \overset{d}{\sim} \mathrm{Gamma}\left(M_j, 1\right)$, $M_1 = N_1 - u_{\mathrm{IN},0}$ and $M_2 = N_2$. Let $\mathbf{h}_{j,\ell 0}$ denote the channel vector between u_0 and BS ℓ in the jth tier, and $\mathbf{f}_{j,\ell}$ denote the beamforming vector at BS ℓ in the jth tier, with $\left|\mathbf{h}_{j,\ell 0}^{\dagger}\mathbf{f}_{j,\ell}\right|^2 \overset{d}{\sim} \mathrm{Gamma}(1,1)$. Let $x_{j,\ell}$ denote the symbol sent from BS ℓ in the jth tier to its scheduled user satisfying $\mathrm{E}\left[x_{j,\ell}x_{j,\ell}^{*}\right] = P_j$. Let $\Phi_{j,1C}$ denote the potential IN macro-BSs of $u_0 \in \mathcal{U}_j$ which do not select it for IN. Let $\Phi_{j,1O}$ denote the interfering macro-BSs of $u_0 \in \mathcal{U}_j$ which are not its potential IN macro-BSs. Let $\Phi_{j,2}$ denote the interfering pico-BSs of $u_0 \in \mathcal{U}_j$. We now discuss the received signal of u_0.

1) Macro-User: The received signal of the typical user $u_0 \in \mathcal{U}_1$ is[6]

$$y_{1,0} = \frac{1}{Y_1^{\frac{\alpha_1}{2}}}\mathbf{h}_{1,00}^{\dagger}\mathbf{f}_{1,0}x_{1,0} + \sum_{\ell\in\Phi_{1,1C}}\frac{1}{D_{1,\ell 0}^{\frac{\alpha_1}{2}}}\mathbf{h}_{1,\ell 0}^{\dagger}\mathbf{f}_{1,\ell}x_{1,\ell} + \sum_{\ell\in\Phi_{1,1O}}\frac{1}{D_{1,\ell 0}^{\frac{\alpha_1}{2}}}\mathbf{h}_{1,\ell 0}^{\dagger}\mathbf{f}_{1,\ell}x_{1,\ell} + \sum_{\ell\in\Phi_{1,2}}\frac{1}{D_{2,\ell 0}^{\frac{\alpha_2}{2}}}\mathbf{h}_{2,\ell 0}^{\dagger}\mathbf{f}_{2,\ell}x_{2,\ell}. \quad (2)$$

Note that $\Phi_{1,1C} \cup \Phi_{1,1O} \cup \{B_{1,0}\} \subseteq \Phi_1$ and $\Phi_{1,2} = \Phi_2$.

2) Pico-User: The received signal of the typical user $u_0 \in \mathcal{U}_2$ is

$$y_{2,0} = \frac{1}{Y_2^{\frac{\alpha_2}{2}}}\mathbf{h}_{2,00}^{\dagger}\mathbf{f}_{2,0}x_{2,0} + \sum_{\ell\in\Phi_{2,1C}}\frac{1}{D_{1,\ell 0}^{\frac{\alpha_1}{2}}}\mathbf{h}_{1,\ell 0}^{\dagger}\mathbf{f}_{1,\ell}x_{1,\ell} + \sum_{\ell\in\Phi_{2,1O}}\frac{1}{D_{1,\ell 0}^{\frac{\alpha_1}{2}}}\mathbf{h}_{1,\ell 0}^{\dagger}\mathbf{f}_{1,\ell}x_{1,\ell} + \sum_{\ell\in\Phi_{2,2}}\frac{1}{D_{2,\ell 0}^{\frac{\alpha_2}{2}}}\mathbf{h}_{2,\ell 0}^{\dagger}\mathbf{f}_{2,\ell}x_{2,\ell}. \quad (3)$$

Note that $\Phi_{2,1C} \cup \Phi_{2,1O} \subseteq \Phi_1$ and $\Phi_{2,2} \cup \{B_{2,0}\} = \Phi_2$.

We now obtain the SIR of the typical user. Under the above IN scheme, $u_0 \in \mathcal{U}_j$ experiences three types of interference: 1) residual aggregated interference $I_{j,1C}$ from its potential IN macro-BSs $\Phi_{j,1C}$ which do not select u_0 for IN, 2) aggregated interference $I_{j,1O}$ from interfering

[5]All the analytical results in this paper hold for $T_1 = T_2 = 1$ and/or $U = 0$.

[6]In this paper, all macro-BSs and pico-BSs are assumed to be active. The same assumption can also be seen in the existing papers (see e.g., [7, 9]). The index of the typical user and its serving BS is 0.

macro-BSs $\Phi_{j,1O}$ which are not its potential IN macro-BSs, and 3) aggregated interference $I_{j,2}$ from all interfering pico-BSs $\Phi_{j,2}$. Specifically, the SIR of the typical user $u_0 \in \mathcal{U}_j$ is given by

$$\mathrm{SIR}_{j,0} = \frac{\frac{P_j}{Y_j^{\alpha_j}} \left| \mathbf{h}_{j,00}^{\dagger} \mathbf{f}_{j,0} \right|^2}{P_1 I_{j,1C} + P_1 I_{j,1O} + P_2 I_{j,2}} \tag{4}$$

where

$$I_{j,1C} = \sum_{\ell \in \Phi_{j,1C}} D_{1,\ell 0}^{-\alpha_1} \left| \mathbf{h}_{1,\ell 0}^{\dagger} \mathbf{f}_{1,\ell} \right|^2, I_{j,1O} = \sum_{\ell \in \Phi_{j,1O}} D_{1,\ell 0}^{-\alpha_1} \left| \mathbf{h}_{1,\ell 0}^{\dagger} \mathbf{f}_{1,\ell} \right|^2, I_{j,2} = \sum_{\ell \in \Phi_{j,2}} D_{2,\ell 0}^{-\alpha_2} \left| \mathbf{h}_{2,\ell 0}^{\dagger} \mathbf{f}_{2,\ell} \right|^2.$$

B. Preliminary Results

In this part, we evaluate some distributions related to the IN scheme, which will be used to calculate the coverage probability in (1). Some of these distributions are based on approximations, the accuracy of which will be verified in Section IV. We first calculate the probability mass function (p.m.f.) of the number of the potential IN users of u_0's serving macro-BS (when $u_0 \in \mathcal{U}_1$), denoted as K_0. The p.m.f. of K_0 depends on the point processes formed by the scheduled macro and pico users, which are related to but not PPPs [21]. For analytical tractability, we approximate the scheduled macro and pico users as two independent PPPs with densities λ_1 and λ_2, respectively.[7] Then, we have the p.m.f. of K_0 as follows.

Lemma 1: The p.m.f. of K_0 is given by

$$\Pr\left(K_0 = k\right) \approx \frac{\bar{L}(T_1, T_2)^k}{k!} \exp\left(-\bar{L}(T_1, T_2)\right) \tag{5}$$

where $\bar{L}(T_1, T_2) = \bar{L}_1(T_1) + \bar{L}_2(T_2)$ with

$$\bar{L}_j(T_j) = 2\pi\lambda_j \int_0^{\infty} r \int_{\left(\frac{P_j}{P_1 T_j}\right)^{\frac{1}{\alpha_j}} r^{\frac{\alpha_1}{\alpha_j}}}^{\left(\frac{P_j}{P_1}\right)^{\frac{1}{\alpha_j}} r^{\frac{\alpha_1}{\alpha_j}}} f_{Y_j}(y) \mathrm{d}y \mathrm{d}r \ , \ j = 1, 2. \tag{6}$$

Here, $f_{Y_j}(y)$ ($j = 1, 2$) are given as follows:

$$f_{Y_1}(y) = \frac{2\pi\lambda_1}{\mathcal{A}_1} y \exp\left(-\pi\left(\lambda_1 y^2 + \lambda_2 \left(\frac{P_2}{P_1}\right)^{\frac{2}{\alpha_2}} y^{\frac{2\alpha_1}{\alpha_2}}\right)\right) \tag{7}$$

$$f_{Y_2}(y) = \frac{2\pi\lambda_2}{\mathcal{A}_2} y \exp\left(-\pi\left(\lambda_1 \left(\frac{P_1}{P_2}\right)^{\frac{2}{\alpha_1}} y^{\frac{2\alpha_2}{\alpha_1}} + \lambda_2 y^2\right)\right) \tag{8}$$

[7]Note that approximating the scheduled users as a homogeneous PPP has been considered in existing papers (see e.g., [21]).

where $\mathcal{A}_j \triangleq \Pr\left(u_0 \in \mathcal{U}_j\right)$ $(j=1,2)$ are given by

$$\mathcal{A}_1 = 2\pi\lambda_1 \int_0^\infty z \exp\left(-\pi\lambda_1 z^2\right) \exp\left(-\pi\lambda_2 \left(\frac{P_2}{P_1}\right)^{\frac{2}{\alpha_2}} z^{\frac{2\alpha_1}{\alpha_2}}\right) \mathrm{d}z \tag{9}$$

$$\mathcal{A}_2 = 2\pi\lambda_2 \int_0^\infty z \exp\left(-\pi\lambda_2 z^2\right) \exp\left(-\pi\lambda_1 \left(\frac{P_1}{P_2}\right)^{\frac{2}{\alpha_1}} z^{\frac{2\alpha_2}{\alpha_1}}\right) \mathrm{d}z. \tag{10}$$

Proof: See Appendix A. ■

Note that $\bar{L}(T_1,T_2)$ represents the average number of IN requests of the scheduled users received by the serving BS of u_0, and $\bar{L}_j(T_j)$ represents the average number of IN requests of the scheduled users in the jth tier received by the serving BS of u_0.

Next, we calculate the p.m.f. of the number of the IN users of u_0's serving macro-BS (when $u_0 \in \mathcal{U}_1$) $u_{\mathrm{IN},0} = \min\left(U, K_0\right)$ based on *Lemma 1*, which is shown as follows.

Lemma 2: The p.m.f. of $u_{\mathrm{IN},0}$ is given by

$$\Pr\left(u_{\mathrm{IN},0}=u\right) = \begin{cases} \Pr\left(K_0=u\right)\ , & \text{for } 0 \le u < U \\ \sum_{k=U}^{\infty} \Pr\left(K_0=k\right)\ , & \text{for } u = U \end{cases}.$$

Let $p_c\left(U,T_1,T_2\right)$ denote the probability that an arbitrary (according to the uniform distribution) potential IN macro-BS of u_0 selects u_0 for IN, referred to as the *IN probabilty*. Note that the event that u_0 sends IN requests and the event that all the other scheduled users send IN requests are dependent. For analytical tractability, we approximate these two events as independent events. Then, we have $p_c\left(U,T_1,T_2\right) \approx \mathrm{E}\left[\min\left\{\frac{U}{K_0+1}, 1\right\}\right]$, which can be calculated as follows.

Lemma 3: The IN probability is given by

$$p_c\left(U,T_1,T_2\right) \approx \exp\left(-\bar{L}(T_1,T_2)\right)\left(\sum_{k=0}^{U-1} \frac{\bar{L}(T_1,T_2)^k}{k!} + U\sum_{k=U}^{\infty} \frac{\bar{L}(T_1,T_2)^k}{(k+1)!}\right).$$

Proof: See Appendix B ■

Note that different potential IN macro-BSs of u_0 selects u_0 for IN dependently (as the numbers of the potential IN users of these macro-BSs are dependent). For analytical tractability, we assume that different potential IN macro-BSs of u_0 select u_0 for IN independently. Using *independent thinning*, u_0's potential IN marcro-BSs can be *approximated* by a homogeneous PPP with density $p_{\bar{c}}\left(U,T_1,T_2\right)\lambda_1$, where $p_{\bar{c}}\left(U,T_1,T_2\right) \triangleq 1 - p_c\left(U,T_1,T_2\right)$.

IV. Coverage Probability–General SIR Threshold Regime

In this section, we investigate the coverage probability in the general SIR threshold regime. By total probability theorem and the preliminary results obtained in Section III-B, we have:

$$\mathcal{S}_1(\beta,U,T_1,T_2)=\sum_{u=0}^{U}\Pr\left(u_{\mathrm{IN},0}=u\right)\int_0^{\infty}\sum_{n=0}^{N_1-u-1}\frac{1}{n!}\sum_{(n_a)_{a=1}^3\in\mathcal{N}_n}\binom{n}{n_1,n_2,n_3}\tilde{\mathcal{L}}_{I_{1,1C}}^{(n_1)}\left(\beta y^{\alpha_1},y,T^{\frac{1}{\alpha_1}}y\right)\times\tilde{\mathcal{L}}_{I_{1,1O}}^{(n_2)}\left(\beta y^{\alpha_1},T_1^{\frac{1}{\alpha_1}}y\right)\tilde{\mathcal{L}}_{I_{1,2}}^{(n_3)}\left(\beta\frac{P_2}{P_1}y^{\alpha_1},\left(\frac{P_2}{P_1}\right)^{\frac{1}{\alpha_2}}y^{\frac{\alpha_1}{\alpha_2}}\right)f_{Y_1}(y)\mathrm{d}y \tag{11}$$

$$\mathcal{S}_2(\beta,U,T_1,T_2)=\int_0^{\infty}\sum_{n=0}^{N_2-1}\frac{1}{n!}\sum_{(n_a)_{a=1}^3\in\mathcal{N}_n}\binom{n}{n_1,n_2,n_3}\tilde{\mathcal{L}}_{I_{2,1C}}^{(n_1)}\left(\beta\frac{P_1}{P_2}y^{\alpha_2},\left(\frac{P_1}{P_2}\right)^{\frac{1}{\alpha_1}}y^{\frac{\alpha_2}{\alpha_1}},\left(\frac{P_1T_2}{P_2}\right)^{\frac{1}{\alpha_1}}y^{\frac{\alpha_2}{\alpha_1}}\right)\times\tilde{\mathcal{L}}_{I_{2,1O}}^{(n_2)}\left(\beta\frac{P_1}{P_2}y^{\alpha_2},\left(\frac{P_1T_2}{P_2}\right)^{\frac{1}{\alpha_1}}y^{\frac{\alpha_2}{\alpha_1}}\right)\tilde{\mathcal{L}}_{I_{2,2}}^{(n_3)}\left(\beta y^{\alpha_2},y\right)f_{Y_2}(y)\mathrm{d}y \tag{12}$$

$$\tilde{\mathcal{L}}_{I_{j,1C}}^{(n)}(U,s,r_{j,1C},r_{j,1O})=\mathcal{L}_{I_{j,1C}}(U,s,r_{j,1C},r_{j,1O})\sum_{(m_a)_{a=1}^n\in\mathcal{M}_n}\frac{n!}{\prod_{a=1}^n m_a!}\prod_{a=1}^n\left(\frac{2\pi}{\alpha_1}p_{\bar{c}}\left(U,T_1,T_2\right)\lambda_1 s^{\frac{2}{\alpha_1}}\times\left(B'\left(1+\frac{2}{\alpha_1},a-\frac{2}{\alpha_1},\frac{1}{1+sr_{j,1C}^{-\alpha_1}}\right)-B'\left(1+\frac{2}{\alpha_1},a-\frac{2}{\alpha_1},\frac{1}{1+sr_{j,1O}^{-\alpha_1}}\right)\right)\right)^{m_a} \tag{13}$$

$$\tilde{\mathcal{L}}_{I_{j,k}}^{(n)}(s,r_{j,k})=\mathcal{L}_{I_{j,k}}(s,r_{j,k})\sum_{(m_a)_{a=1}^n\in\mathcal{M}_n}\frac{n!}{\prod_{a=1}^n m_a!}\prod_{a=1}^n\left(B'\left(1+\frac{2}{\alpha_{J(k)}},a-\frac{2}{\alpha_{J(k)}},\frac{1}{1+\frac{s}{r_{j,k}^{\alpha_{J(k)}}}}\right)\times\frac{2\pi\lambda_{J(k)}}{\alpha_{J(k)}}s^{\frac{2}{\alpha_{J(k)}}}\right)^{m_a} \tag{14}$$

$$\mathcal{L}_{I_{j,1C}}(U,s,r_{j,1C},r_{j,1O})=\exp\left(-\left(B'\left(\frac{2}{\alpha_1},1-\frac{2}{\alpha_1},\frac{1}{1+sr_{j,1C}^{-\alpha_1}}\right)-B'\left(\frac{2}{\alpha_1},1-\frac{2}{\alpha_1},\frac{1}{1+sr_{j,1O}^{-\alpha_1}}\right)\right)\times\frac{2\pi}{\alpha_1}p_{\bar{c}}\left(U,T_1,T_2\right)\lambda_1 s^{\frac{2}{\alpha_1}}\right) \tag{15}$$

$$\mathcal{L}_{I_{j,k}}(s,r_{j,k})=\exp\left(-\frac{2\pi\lambda_{J(k)}}{\alpha_{J(k)}}s^{\frac{2}{\alpha_{J(k)}}}B'\left(\frac{2}{\alpha_{J(k)}},1-\frac{2}{\alpha_{J(k)}},\frac{1}{1+\frac{s}{r_{j,k}^{\alpha_{J(k)}}}}\right)\right) \tag{16}$$

Theorem 1 (Coverage Probability): Under design parameters U, T_1 and T_2, we have: 1) coverage probability of a macro-user: $\mathcal{S}_1\left(\beta,U,T_1,T_2\right)\triangleq\Pr\left(\mathrm{SIR}_0>\beta|u_0\in\mathcal{U}_1\right)$, given in (11); 2)

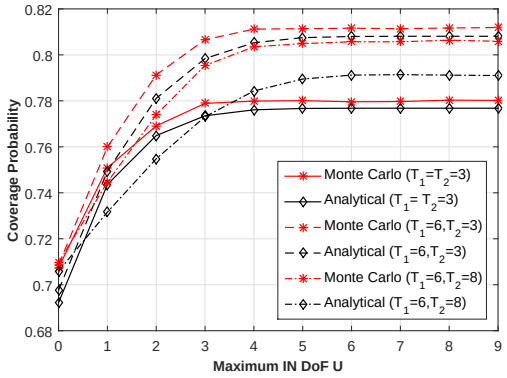

Fig. 2. Coverage probability versus maximum IN DoF. $N_1 = 10$, $N_2 = 8$, $\beta = 10$ dB, $\alpha_1 = 4.5$, $\alpha_2 = 4.7$, $\frac{P_1}{P_2} = 15$ dB, $\lambda_1 = 0.0005$ nodes/m^2, and $\lambda_2 = 0.001$ nodes/m^2. Note that when T_1 and T_2 are small, the coverage probability increases with T_1 and T_2, as the number of potential IN users benefiting from IN increases; when T_1 and T_2 are large, the coverage probability decreases with T_1 and T_2, as the chance for worse potential IN users being selected for IN decreases.

coverage probability of a pico-user: $\mathcal{S}_2\left(\beta, U, T_1, T_2\right) \triangleq \Pr\left(\mathrm{SIR}_0 > \beta | u_0 \in \mathcal{U}_2\right)$, given in (12); 3) overall coverage probability $\mathcal{S}\left(\beta, U, T_1, T_2\right) = \mathcal{A}_1\mathcal{S}_1(\beta, U, T_1, T_2) + \mathcal{A}_2\mathcal{S}_2(\beta, U, T_1, T_2)$, where $\mathcal{A}_j \triangleq \Pr\left(u_0 \in \mathcal{U}_j\right)$ $(j = 1, 2)$ are given in (9) and (10). Here, $\tilde{\mathcal{L}}^{(n)}_{I_{j,1C}}\left(U, s, r_{j,1C}, r_{j,1O}\right)$ and $\tilde{\mathcal{L}}^{(n)}_{I_{j,k}}(s, r_{j,k})$ $(k \in \{1O, 2\})$ are given in (13) and (14), respectively, where[8] $\mathcal{L}_{I_{j,1C}}\left(U, s, r_{j,1C}, r_{j,1O}\right)$ and $\mathcal{L}_{I_{j,k}}(s, r_{j,k})$ are given in (15) and (16) (with $J(1O) = 1$ and $J(2) = 2$), respectively. Moreover, $B'(a, b, z) \triangleq \int_z^1 u^{a-1}(1-u)^{b-1}\mathrm{d}u$ $(0 < z < 1)$, $\mathcal{N}_n \triangleq \{(n_a)_{a=1}^3 | n_a \in \mathbb{N}^0, \sum_{a=1}^3 n_a = n\}$, and $\mathcal{M}_n \triangleq \{(m_a)_{a=1}^n | m_a \in \mathbb{N}^0, \sum_{a=1}^3 a \cdot m_a = n\}$, where $\mathbb{N}^0$ denotes the set of nonnegative integers.

Proof: See Appendix C. ■

Theorem 1 allows us to easily evaluate the coverage probability. Fig. 2 plots the coverage probability versus the IN DoF U. We see from Fig. 2 that the "Analytical" curves, which are plotted using $\mathcal{S}\left(\beta, U, T_1, T_2\right)$ in *Theorem 1*, are reasonably close to the "Monte Carlo" curves (the error is no larger than 2.03%), although *Theorem 1* is obtained based on some approximations (cf. Section III-B). Later, we shall consider the optimization of U for given T_1 and T_2.[9]

[8] $\mathcal{L}_I$ denotes the Laplace transform of the aggregated interference I.

[9] The coverage probability can be further improved by jointly adjusting T_1 and T_2. We shall consider the optimization of T_1 and T_2 in the future work.

V. Asymptotic Coverage Probability Analysis–Low SIR Threshold Regime

In this section, we investigate the complement of the coverage probability, i.e., outage probability of the IN scheme in the low SIR threshold regime, i.e., $\beta \to 0$.

A. Asymptotic Outage Probability Analysis

In this part, we analyze the asymptotic outage probability $\Pr(\mathrm{SIR}_0 < \beta)$ of the IN scheme when $\beta \to 0$. First, we define the *order gain* of the outage probability [22]:

$$d \triangleq \lim_{\beta \to 0} \frac{\log \Pr(\mathrm{SIR}_0 < \beta)}{\log \beta}. \tag{17}$$

Then, we define the *coefficient* of the asymptotic outage probability: $\lim_{\beta\to 0} \frac{\Pr(\mathrm{SIR}_0<\beta)}{\beta^d}$. Recently, a tractable approach has been proposed in [23] to characterize the order gain for a class of communication schemes in wireless networks which satisfy certain conditions. However, this approach does not provide tractable analytical expressions for the coefficient of the asymptotic outage probability for most of the schemes using multiple antennas in this class. By utilizing series expansion of some special functions and dominated convergence theorem, we characterize both the order gain and the coefficient of the asymptotic outage probability of the IN scheme in multi-antenna HetNets, which are presented as follows:

Theorem 2 (Asymptotic Outage Probability): Under design parameters U, T_1 and T_2, when $\beta \to 0$, we have:[10] 1) outage probability of a macro-user: $1-\mathcal{S}_1(\beta, U, T_1, T_2) \overset{\beta\to 0}{\sim} b_1(U, T_1, T_2)\, \beta^{N_1-U}$; 2) outage probability of a pico-user: $1-\mathcal{S}_2(\beta, U, T_1, T_2) \overset{\beta\to 0}{\sim} b_2(U, T_1, T_2)\, \beta^{N_2}$; 3) overall outage probability: $1-\mathcal{S}(\beta, U, T_1, T_2) \overset{\beta\to 0}{\sim} b(U, T_1, T_2)\, \beta^{\min\{N_1-U, N_2\}}$, where

$$b(U, T_1, T_2) = \begin{cases} b_2(U, T_1, T_2), & U < N_1 - N_2 \\ b_1(U, T_1, T_2) + b_2(U, T_1, T_2), & U = N_1 - N_2 \\ b_1(U, T_1, T_2), & U > N_1 - N_2 \end{cases}.$$

Here, $b_j(U, T_1, T_2)$ is given in (18) with $U_j = U$ and $\mathcal{P}_j = \Pr(u_{\mathrm{IN},0} = U)$ if $j = 1$ and $T_1, T_2 > 1$; $U_j = 0$ and $\mathcal{P}_j = 1$, otherwise. Moreover, $b_2(U, T_1, T_2)$ decreases with U.

Proof: See Appendix D. ∎

[10] $f(\beta) \overset{\beta\to 0}{\sim} g(\beta)$ means $\lim_{\beta\to 0} \frac{f(\beta)}{g(\beta)} = 1$.

$$
\begin{aligned}
&b_j\left(U,T_1,T_2\right)\\
&=\sum_{(n_a)_{a=1}^3\in\mathcal{N}_{N_j-U_j}}\ \sum_{(m_a)_{a=1}^{n_1}\in\mathcal{M}_{n_1}}\ \sum_{(p_a)_{a=1}^{n_2}\in\mathcal{M}_{n_2}}\ \sum_{(q_a)_{a=1}^{n_3}\in\mathcal{M}_{n_3}}\left(\int_0^\infty y^{\frac{2\alpha_j}{\alpha_1}\left(\sum_{a=1}^{n_1}m_a+\sum_{a=1}^{n_2}p_a\right)+\frac{2\alpha_j}{\alpha_2}\sum_{a=1}^{n_2}q_a}f_{Y_j}(y)\mathrm{d}y\right)\\
&\times\left(\prod_{a=1}^{n_2}\left(\left(\frac{1}{T_j}\right)^{a-\frac{2}{\alpha_1}}\right)^{p_a}\right)\left(\prod_{a=1}^{n_1}\frac{1}{m_a!}\left(\frac{\frac{2}{\alpha_1}\pi\lambda_1}{a-\frac{2}{\alpha_1}}\left(\frac{P_1}{P_j}\right)^{\frac{2}{\alpha_1}}\right)^{m_a}\right)\left(\prod_{a=1}^{n_2}\frac{1}{p_a!}\left(\frac{\frac{2}{\alpha_1}\pi\lambda_1}{a-\frac{2}{\alpha_1}}\left(\frac{P_1}{P_j}\right)^{\frac{2}{\alpha_1}}\right)^{p_a}\right)\\
&\times\left(\prod_{a=1}^{n_3}\frac{1}{q_a!}\left(\frac{\frac{2}{\alpha_2}\pi\lambda_2}{a-\frac{2}{\alpha_2}}\left(\frac{P_2}{P_j}\right)^{\frac{2}{\alpha_2}}\right)^{q_a}\right)\left(\prod_{a=1}^{n_1}\left(p_{\bar{c}}\left(U,T_1,T_2\right)\left(1-\left(\frac{1}{T_j}\right)^{a-\frac{2}{\alpha_1}}\right)\right)^{m_a}\right)\mathcal{P}_j \qquad (18)
\end{aligned}
$$

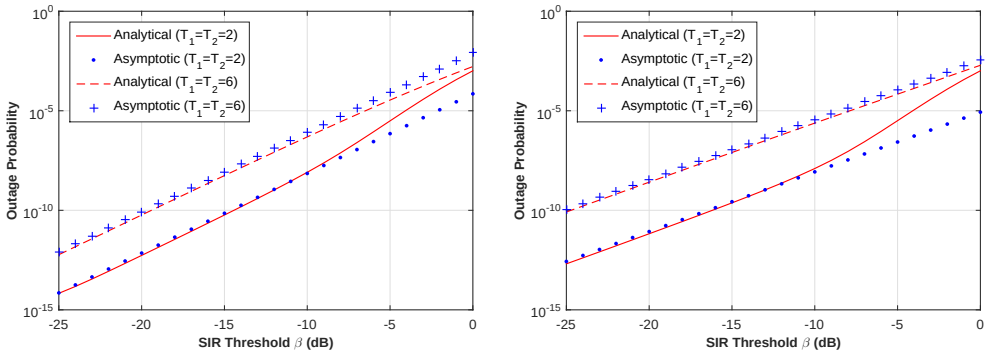

(a) $U=6$ (b) $U=7$

Fig. 3. Outage probability versus SIR threshold in the low SIR threshold regime. $N_1=10$, $N_2=8$, $\alpha_1=4.5$, $\alpha_2=4.7$, $\frac{P_1}{P_2}=15$ dB, $\lambda_1=0.0005$ nodes/m^2, and $\lambda_2=0.001$ nodes/m^2.

Note that the IN scheme has three design parameters: the maximum IN DoF (i.e., U) and the IN thresholds (i.e., T_1 and T_2). From *Theorem 2*, we clearly see that the maximum IN DoF and the IN thresholds affect the asymptotic behavior of the outage probability in dramatically different ways. Specifically, the maximum IN DoF U can affect the order gain, while the IN thresholds can only affect the coefficient. In addition, we see that U affects the order gain of the asymptotic outage probability through affecting the order gain of the asymptotic macro-user outage probability. On the other hand, in this paper, IN is only performed at macro-BSs, and U is the upper bound of the actual DoF for IN in the ZFBF precoder (which is *random* due to the randomness of the network topology). Therefore, the result of the order gain in *Theorem 2* extends the existing order gain result in *single-tier* cellular networks where the DoF for IN in the ZFBF precoder is *deterministic* [15].

Fig. 3 plots the outage probability versus the SIR threshold in the low SIR threshold regime. We see from Fig. 3 that when the SIR threshold is small, the "Analytical" curves, which are plotted using *Theorem 1*, are reasonably close to the "Asymptotic" curves, which are plotted using *Theorem 2*. In addition, from Fig. 3, we clearly see that the outage probability curves with the same maximum IN DoF U have the same slope (indicating the same order gain), and there is a shift between two outage probability curves with the same U but different (T_1, T_2) (indicating different coefficients). Therefore, Fig. 3 verifies *Theorem 2*.

B. Asymptotic Outage Probability Optimization

From *Theorem 2*, we know that U has a larger impact on the asymptotic outage probability than the IN thresholds. In this part, we characterize the optimal maximum IN DoF $U^*(\beta, T_1, T_2)$ which minimizes the asymptotic outage probability given in *Theorem 2* (i.e., maximizes the asymptotic coverage probability) for given thresholds T_1 and T_2, i.e.,

$$U^*(\beta, T_1, T_2) \triangleq \arg \min_{U \in \{0,1,\ldots,N_1-1\}} b\left(U, T_1, T_2\right) \beta^{\min\{N_1-U, N_2\}} . \tag{19}$$

Lemma 4 (Optimality Property of $U^*(\beta, T_1, T_2)$): $\exists \bar{\beta} > 0$ such that for all $\beta < \bar{\beta}$, we have[11]

$$U^*(\beta, T_1, T_2) = \begin{cases} N_1 - N_2 - 1, & \text{if } b_2\left(N_1 - N_2 - 1, T_1, T_2\right) < \\ & \qquad b_1\left(N_1 - N_2, T_1, T_2\right) + b_2\left(N_1 - N_2, T_1, T_2\right) \cdot \\ N_1 - N_2, & \text{otherwise} \end{cases}$$

Proof: See Appendix E. ■

Lemma 4 indicates that in the low threshold regime, the IN scheme achieves the optimal asymptotic outage probability when reserving N_2 or $N_2 + 1$ DoF at each macro-BS to boost the desired signal to its scheduled user, which is comparable to the N_2 DoF used at each pico-BS to boost the desired signal to its scheduled user. The reason is that in the low threshold regime, the network performance is mainly limited by the worst users. Balancing the DoF for boosting signals to all the users effectively improves the performance of the worst users. Fig. 4 plots the outage probability versus the maximum IN DoF in the small SIR threshold regime. From Fig. 4, we can see that $U^*(\beta, T_1, T_2) = N_1 - N_2 - 1$ or $N_1 - N_2$ at small β. This verifies *Lemma 4*.

[11] *Lemma 4* is similar to *Theorem 3* of our previous work [14]. The reason is that the two interference management schemes in this paper and [14] are both based on IN. One difference is that the proposed scheme in this paper aims to improve the performance of all users with low SIIR, while the scheme in [14] only improves the performance of offloaded users.

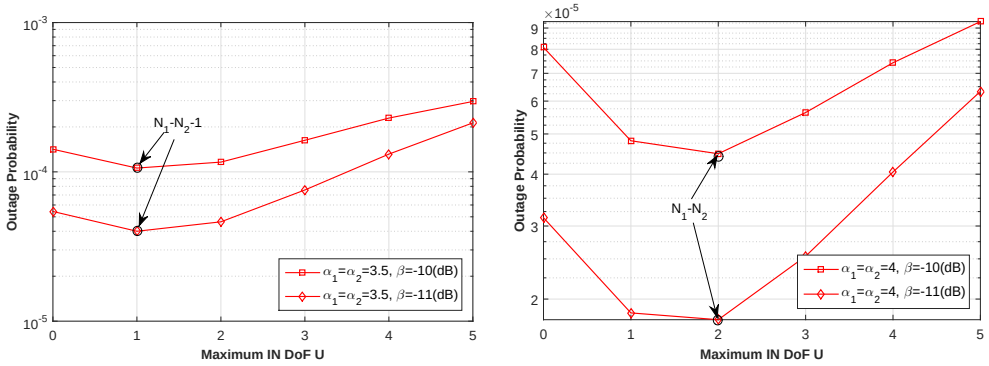

(a) $U = 1$ (b) $U = 2$

Fig. 4. Outage probability versus maximum IN DoF in the small SIR threshold regime. $N_1 = 6$, $N_2 = 4$, $T_1 = T_2 = 1.8$ $\frac{P_1}{P_2} = 15$ dB, $\lambda_1 = 0.0005$ nodes/m^2, and $\lambda_2 = 0.001$ nodes/m^2.

VI. Asymptotic Coverage Probability Analysis–High SIR Threshold Regime

In this section, we investigate the coverage probability of the IN scheme in the high SIR threshold regime, i.e., $\beta \to \infty$.

A. Asymptotic Coverage Probability Analysis

In this part, we analyze the asymptotic coverage probability of the IN scheme when $\beta \to \infty$. First, we define the *order gain* of the coverage probability as follows:

$$d_c \triangleq \lim_{\beta \to \infty} \frac{\Pr\left(\mathrm{SIR}_0 > \beta\right)}{\log \beta}. \tag{20}$$

Then, we define the *coefficient* of the asymptotic coverage probability: $\lim_{\beta\to\infty} \frac{\Pr(\mathrm{SIR}_0>\beta)}{\beta^{d_c}}$. In the following, we analyze the asymptotic coverage probability in two scenarios, i.e., $\alpha_1 \neq \alpha_2$ and $\alpha_1 = \alpha_2$.

When $\alpha_1 \neq \alpha_2$, it turns out to be difficult to obtain the expression of the asymptotic coverage probability. Thus, we derive lower and upper bounds of the asymptotic coverage probability, which are given in the following theorem.

Theorem 3 (Asymptotic Coverage Probability When $\alpha_1 \neq \alpha_2$): Under design parameters U, T_1 and T_2, when $\alpha_1 \neq \alpha_2$ and $\beta \to \infty$, we have:[12] 1) coverage probability of a macro-user: $\mathcal{S}_1\left(\beta, U, T_1, T_2\right) \overset{\beta\to\infty}{\sim} \tilde{\mathcal{S}}_1\left(\beta, U, T_1, T_2\right)$, where $\xi_1 \beta^{-\frac{2}{\alpha_1}\frac{\alpha_{\max}}{\alpha_{\min}}} < \tilde{\mathcal{S}}_1\left(\beta, U, T_1, T_2\right) < \eta_1\left(U, T_1, T_2\right)\beta^{-\frac{2}{\alpha_1}}$;

[12] $f(\beta) \overset{\beta\to\infty}{\sim} g(\beta)$ means $\lim_{\beta\to\infty} \frac{f(\beta)}{g(\beta)} = 1$.

$$\eta_1\left(U,T_1,T_2\right)=\frac{\pi\lambda_1}{\mathcal{A}_1}\sum_{u=0}^{U}\Pr\left(u_{\mathrm{IN},0}=u\right)\sum_{n=0}^{N_1-u-1}\frac{1}{n!}\sum_{n_2=0}^{n}\binom{n}{n_2}\sum_{\left(p_a\right)_{a=1}^{n_2}\in\mathcal{M}_{n_2}}\sum_{\left(q_a\right)_{a=1}^{n-n_2}\in\mathcal{M}_{n-n_2}}\frac{n_2!}{\prod_{a=1}^{n_2}p_a!}$$
$$\times\prod_{a=1}^{n_2}\left(\frac{2\pi}{\alpha_1}\lambda_1\mathrm{B}\left(1+\frac{2}{\alpha_1},a-\frac{2}{\alpha_1}\right)\right)^{p_a}\frac{(n-n_2)!}{\prod_{a=1}^{n-n_2}q_a!}\prod_{a=1}^{n-n_2}\left(\frac{2\pi}{\alpha_2}\lambda_2\left(\frac{P_2}{P_1}\right)^{\frac{2}{\alpha_2}}\mathrm{B}\left(1+\frac{2}{\alpha_2},a-\frac{2}{\alpha_2}\right)\right)^{q_a}$$
$$\times\left(\frac{2\pi\lambda_1}{\alpha_1}\mathrm{B}\left(\frac{2}{\alpha_1},1-\frac{2}{\alpha_1}\right)\right)^{-\sum_{a=1}^{n_2}p_a-\frac{\alpha_1}{\alpha_2}\sum_{a=1}^{n-n_2}q_a-1}\Gamma\left(\sum_{a=1}^{n_2}p_a+\frac{\alpha_1}{\alpha_2}\sum_{a=1}^{n-n_2}q_a+1\right)\tag{21}$$

$$\eta_2=\frac{\pi\lambda_2}{\mathcal{A}_2}\sum_{n=0}^{N_2-1}\frac{1}{n!}\sum_{n_2=0}^{n}\binom{n}{n_2}\sum_{\left(p_a\right)_{a=1}^{n_2}\in\mathcal{M}_{n_2}}\sum_{\left(q_a\right)_{a=1}^{n-n_2}\in\mathcal{M}_{n-n_2}}\frac{n_2!}{\prod_{a=1}^{n_2}p_a!}\frac{(n-n_2)!}{\prod_{a=1}^{n-n_2}q_a!}$$
$$\times\prod_{a=1}^{n_2}\left(\frac{2\pi}{\alpha_1}\lambda_1\left(\frac{P_1}{P_2}\right)^{\frac{2}{\alpha_1}}\mathrm{B}\left(1+\frac{2}{\alpha_1},a-\frac{2}{\alpha_1}\right)\right)^{p_a}\prod_{a=1}^{n-n_2}\left(\frac{2\pi}{\alpha_2}\lambda_2\mathrm{B}\left(1+\frac{2}{\alpha_2},a-\frac{2}{\alpha_2}\right)\right)^{q_a}$$
$$\times\left(\frac{2\pi\lambda_1}{\alpha_2}\mathrm{B}\left(\frac{2}{\alpha_2},1-\frac{2}{\alpha_2}\right)\right)^{-\frac{\alpha_2}{\alpha_1}\sum_{a=1}^{n_2}p_a-\sum_{a=1}^{n-n_2}q_a-1}\Gamma\left(\frac{\alpha_2}{\alpha_1}\sum_{a=1}^{n_2}p_a+\sum_{a=1}^{n-n_2}q_a+1\right)\tag{22}$$

$$\xi_1=\frac{\pi\lambda_1\alpha_{\max}}{\mathcal{A}_1\alpha_1}\left(\frac{2\pi\lambda_1}{\alpha_1}\mathrm{B}\left(\frac{2}{\alpha_1},1-\frac{2}{\alpha_1}\right)+\frac{2\pi\lambda_2}{\alpha_2}\left(\frac{P_2}{P_1}\right)^{\frac{2}{\alpha_2}}\mathrm{B}\left(\frac{2}{\alpha_2},1-\frac{2}{\alpha_2}\right)\right)^{-\frac{\alpha_{\max}}{\alpha_1}}\Gamma\left(\frac{\alpha_{\max}}{\alpha_1}\right)\tag{23}$$

$$\xi_2=\frac{\pi\lambda_2\alpha_{\max}}{\mathcal{A}_2\alpha_2}\left(\frac{2\pi\lambda_1}{\alpha_1}\left(\frac{P_1}{P_2}\right)^{\frac{2}{\alpha_1}}\mathrm{B}\left(\frac{2}{\alpha_1},1-\frac{2}{\alpha_1}\right)+\frac{2\pi\lambda_2}{\alpha_2}\mathrm{B}\left(\frac{2}{\alpha_2},1-\frac{2}{\alpha_2}\right)\right)^{-\frac{\alpha_{\max}}{\alpha_2}}\Gamma\left(\frac{\alpha_{\max}}{\alpha_2}\right)\tag{24}$$

---

2) coverage probability of a pico-user: $\mathcal{S}_2\left(\beta,U,T_1,T_2\right)\overset{\beta\to\infty}{\sim}\tilde{\mathcal{S}}_2\left(\beta,U,T_1,T_2\right)$, where $\xi_2\beta^{-\frac{2}{\alpha_2}\frac{\alpha_{\max}}{\alpha_{\min}}}<\tilde{\mathcal{S}}_2\left(\beta,U,T_1,T_2\right)<\eta_2\beta^{-\frac{2}{\alpha_2}}$; 3) overall coverage probability: $\mathcal{S}\left(\beta,U,T_1,T_2\right)\overset{\beta\to\infty}{\sim}\tilde{\mathcal{S}}\left(\beta,U,T_1,T_2\right)$, where $c^{\mathrm{lb}}\beta^{-\frac{2}{\alpha_{\min}}}<\tilde{\mathcal{S}}\left(\beta,U,T_1,T_2\right)<c^{\mathrm{ub}}\left(U,T_1,T_2\right)\beta^{-\frac{2}{\alpha_{\max}}}$. Here, $\alpha_{\min}=\min\left\{\alpha_1,\alpha_2\right\}$, $\alpha_{\max}=\max\left\{\alpha_1,\alpha_2\right\}$, $\mathrm{B}(a,b)\triangleq\int_0^1 t^{a-1}(1-t)^{b-1}\mathrm{d}t$ is the beta function, $\eta_1\left(U,T_1,T_2\right)$ and η_2 are given in (21) and (22), respectively, ξ_j $(j=1,2)$ are given in (23) and (24), respectively, and

$$c^{\mathrm{ub}}\left(U,T_1,T_2\right)=\begin{cases}\eta_1\left(U,T_1,T_2\right), & \alpha_1>\alpha_2\\ \eta_2, & \alpha_1<\alpha_2\end{cases},\ c^{\mathrm{lb}}=\begin{cases}\xi_1, & \alpha_1>\alpha_2\\ \xi_2, & \alpha_1<\alpha_2\end{cases}.$$

Proof: See Appendix F. ■

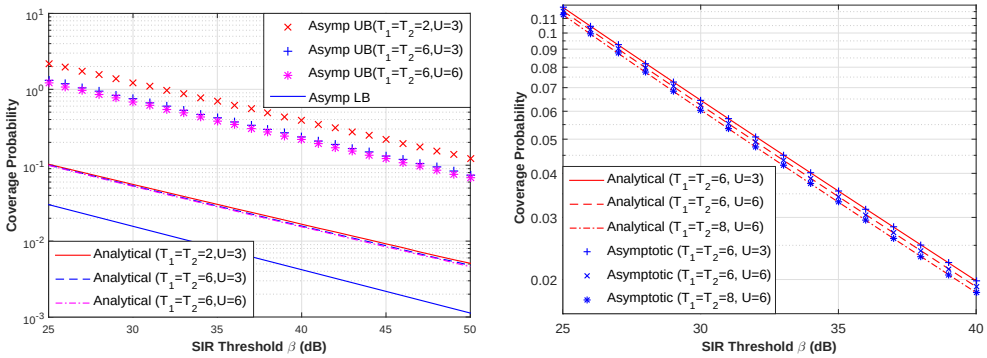

(a) $\alpha_1 = 4$, $\alpha_2 = 3.5$ (b) $\alpha_1 = \alpha_2 = 4$

Fig. 5. Coverage probability versus SIR threshold in the high SIR threshold regime. $N_1 = 10$, $N_2 = 8$, $\frac{P_1}{P_2} = 15$ dB, $\lambda_1 = 0.0005$ nodes/m^2, and $\lambda_2 = 0.001$ nodes/m^2.

When $\alpha_1 = \alpha_2$, we derive the asymptotic coverage probability, which is given below.

Theorem 4 (Asymptotic Coverage Probability When $\alpha_1 = \alpha_2$): Under design parameters U, T_1 and T_2, when $\alpha_1 = \alpha_2 = \alpha$ and $\beta \to \infty$, we have: 1) coverage probability of a macro-user: $\mathcal{S}_1(\beta, U, T_1, T_2) \overset{\beta\to\infty}{\sim} c_1(U, T_1, T_2)\beta^{-\frac{2}{\alpha}}$, where $c_1(U, T_1, T_2)$ is given in (25); 2) coverage probability of a pico-user: $\mathcal{S}_2(\beta, U, T_1, T_2) \overset{\beta\to\infty}{\sim} c_2(T_1, T_2)\beta^{-\frac{2}{\alpha}}$, where $c_2(T_1, T_2)$ is given in (26); 3) overall coverage probability: $\mathcal{S}(\beta, T_1, T_2) \overset{\beta\to\infty}{\sim} (\mathcal{A}_1 c_1(U, T_1, T_2) + \mathcal{A}_2 c_2(T_1, T_2))\beta^{-\frac{2}{\alpha}}$.

Proof: See Appendix G. ■

From *Theorem 3* and *Theorem 4*, we clearly see that when $\alpha_1 \neq \alpha_2$, the order gains of the lower and upper bounds on the asymptotic coverage probability do not depend on U, T_1 and T_2; when $\alpha_1 = \alpha_2$, the order gain of the asymptotic coverage probability does not depend on U, T_1 and T_2. Hence, for arbitrary α_1 and α_2, the design parameters U, T_1 and T_2 do not affect the order gain of the asymptotic coverage probability in both scenarios. In other words, the IN scheme does not provide order-wise performance improvement compared to the simple beamforming scheme when $\beta \to \infty$. In addition, T_1 and T_2 affect the coefficient of the upper bound on the asymptotic coverage probability when $\alpha_1 \neq \alpha_2$ and the coefficient of the asymptotic coverage probability when $\alpha_1 = \alpha_2$. While, U affects the coefficient of the upper bound on the asymptotic coverage probability when $\alpha_1 \neq \alpha_2$ and the coefficient the asymptotic coverage probability when $\alpha_1 = \alpha_2$, through affecting the upper bound on the asymptotic coverage probability of a macro-user when $\alpha_1 \neq \alpha_2$ and the asymptotic coverage probability of a macro-user when $\alpha_1 = \alpha_2$, respectively.

$$c_1\left(U,T_1,T_2\right)=\frac{\pi\lambda_1}{\mathcal{A}_1}\sum_{u=0}^{U}\Pr\left(u_{\mathrm{IN},0}=u\right)\sum_{n=0}^{N_1-u-1}\frac{1}{n!}\sum_{n_2=0}^{n}\binom{n}{n_2}\sum_{(p_a)_{a=1}^{n_2}\in\mathcal{M}_{n_2}}\sum_{(q_a)_{a=1}^{n-n_2}\in\mathcal{M}_{n-n_2}}\frac{n_2!}{\prod_{a=1}^{n_2}p_a!}$$
$$\times\prod_{a=1}^{n_2}\left(\frac{2\pi}{\alpha}\lambda_1\mathrm{B}\left(1+\frac{2}{\alpha},a-\frac{2}{\alpha}\right)\right)^{p_a}\frac{(n-n_2)!}{\prod_{a=1}^{n-n_2}q_a!}\prod_{a=1}^{n-n_2}\left(\frac{2\pi}{\alpha}\lambda_2\left(\frac{P_2}{P_1}\right)^{\frac{2}{\alpha}}\mathrm{B}\left(1+\frac{2}{\alpha},a-\frac{2}{\alpha}\right)\right)^{q_a}$$
$$\times\left(\frac{2\pi}{\alpha}\lambda_1\mathrm{B}\left(\frac{2}{\alpha},1-\frac{2}{\alpha}\right)+\frac{2\pi}{\alpha}\lambda_2\left(\frac{P_2}{P_1}\right)^{\frac{2}{\alpha}}\mathrm{B}\left(\frac{2}{\alpha},1-\frac{2}{\alpha}\right)\right)^{-\frac{\alpha}{\alpha}\sum_{a=1}^{n_2}p_a-\frac{\alpha}{\alpha}\sum_{a=1}^{n-n_2}q_a-\frac{\alpha}{\alpha}}$$
$$\times\Gamma\left(\sum_{a=1}^{n_2}p_a+\sum_{a=1}^{n-n_2}q_a+1\right) \tag{25}$$

$$c_2\left(T_1,T_2\right)=\frac{\pi\lambda_2}{\mathcal{A}_2}\sum_{n=0}^{N_2-1}\frac{1}{n!}\sum_{n_2=0}^{n}\binom{n}{n_2}\sum_{(p_a)_{a=1}^{n_2}\in\mathcal{M}_{n_2}}\sum_{(q_a)_{a=1}^{n-n_2}\in\mathcal{M}_{n-n_2}}\frac{n_2!}{\prod_{a=1}^{n_2}p_a!}\frac{(n-n_2)!}{\prod_{a=1}^{n-n_2}q_a!}$$
$$\times\prod_{a=1}^{n_2}\left(\frac{2\pi}{\alpha}\lambda_1\left(\frac{P_1}{P_2}\right)^{\frac{2}{\alpha}}\mathrm{B}\left(1+\frac{2}{\alpha},a-\frac{2}{\alpha}\right)\right)^{p_a}\prod_{a=1}^{n-n_2}\left(\frac{2\pi}{\alpha}\lambda_2\mathrm{B}\left(1+\frac{2}{\alpha},a-\frac{2}{\alpha}\right)\right)^{q_a}$$
$$\times\left(\frac{2\pi}{\alpha}\lambda_1\left(\frac{P_1}{P_2}\right)^{\frac{2}{\alpha}}\mathrm{B}\left(\frac{2}{\alpha},1-\frac{2}{\alpha}\right)+\frac{2\pi}{\alpha}\lambda_2\mathrm{B}\left(\frac{2}{\alpha},1-\frac{2}{\alpha}\right)\right)^{-\frac{\alpha}{\alpha}\sum_{a=1}^{n_2}p_a-\frac{\alpha}{\alpha}\sum_{a=1}^{n-n_2}q_a-\frac{\alpha}{\alpha}}$$
$$\times\Gamma\left(\sum_{a=1}^{n_2}p_a+\sum_{a=1}^{n-n_2}q_a+1\right) \tag{26}$$

Fig. 5 plots the coverage probability versus the SIR threshold in the high SIR threshold regime for $\alpha_1\neq\alpha_2$ and $\alpha_1=\alpha_2$, respectively. We see from Fig. 5(a) that when $\alpha_1\neq\alpha_2$, the "Analytical" curves, which are plotted using *Theorem 1*, are bounded by the corresponding "Asymptotic" upper bound curves and lower bound curve, which are plotted using *Theorem 3*. Note that there is only one "Asymptotic" lower bound curve, as the asymptotic lower bound is independent of U and (T_1,T_2). In addition, from Fig. 5(a), we clearly see that the coverage probability curves with different maximum IN DoF U or (T_1,T_2) have slightly different slopes (indicating different order gains), and there is a small shift between any two coverage probability curves with the different U or (T_1,T_2) (indicating different coefficients). On the other hand, we see from Fig. 5(b) that when $\alpha_1=\alpha_2$, the "Analytical" curves, which are plotted using $\mathcal{S}\left(\beta,U,T_1,T_2\right)$ in *Theorem 1*, are reasonably close to the "Asymptotic" curves, which are plotted using *Theorem 4*. In addition,

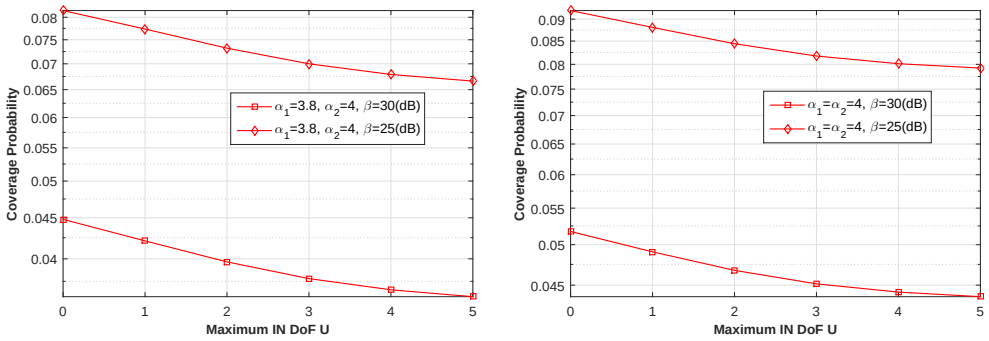

(a) $\alpha_1 \neq \alpha_2$ (b) $\alpha_1 = \alpha_2$

Fig. 6. Coverage probability versus maximum IN DoF in the high SIR threshold regime. $N_1 = 6$, $N_2 = 4$, $T_1 = T_2 = 4$ $\frac{P_1}{P_2} = 15$ dB, $\lambda_1 = 0.0005$ nodes/m^2, and $\lambda_2 = 0.001$ nodes/m^2.

from Fig. 5(b), we clearly see that the coverage probability curves with different maximum IN DoF U or (T_1, T_2) have the same slope (indicating the same order gain), and there is a shift between any two coverage probability curves with the different U or (T_1, T_2) (indicating different coefficients). Therefore, Fig. 5 verifies *Theorem 3* and *Theorem 4*.

B. Asymptotic Coverage Probability Optimization

In this part, we characterize the optimal maximum IN DoF $U^*(\beta, T_1, T_2)$ which maximizes the upper bound[13] of the asymptotic coverage probability given in *Theorem 3* when $\alpha_1 \neq \alpha_2$ and the asymptotic coverage probability given in *Theorem 4* when $\alpha_1 = \alpha_2$, for given thresholds T_1 and T_2, i.e.,

$$U^*(\beta, T_1, T_2) \triangleq \begin{cases} \arg\max_{U\in\{0,1,\ldots,N_1-1\}} c^{\text{ub}}(U, T_1, T_2)\, \beta^{-\frac{2}{\alpha_{\max}}}, & \alpha_1 \neq \alpha_2 \\ \arg\max_{U\in\{0,1,\ldots,N_1-1\}} \left(c_1(U, T_1, T_2) + c_2(T_1, T_2)\right) \beta^{-\frac{2}{\alpha}}, & \alpha_1 = \alpha_2 \end{cases}$$
$$= \begin{cases} \arg\max_{U\in\{0,1,\ldots,N_1-1\}} c^{\text{ub}}(U, T_1, T_2), & \alpha_1 \neq \alpha_2 \\ \arg\max_{U\in\{0,1,\ldots,N_1-1\}} c_1(U, T_1, T_2), & \alpha_1 = \alpha_2 \end{cases}. \quad (27)$$

Lemma 5 (Optimality Property of $U^*(\beta, T_1, T_2)$): There exists $\underline{\beta} < \infty$ such that for all $\beta > \underline{\beta}$, we have $U^*(\beta, T_1, T_2) = 0$ for arbitrary α_1 and α_2.

Proof: See Appendix H. ■

[13]Note that U does not affect the lower bound of the asymptotic coverage probability given in *Theorem 3*.

Lemma 5 indicates that performing IN will not improve the asymptotic coverage probability in the high SIR threshold regime. The reason is that in the high SIR threshold regime, the overall coverage probability is mainly contributed by cell center users, which have much better performance than cell edge users. Using all N_1 DoF at each macro-BS to boost the desired signal to its scheduled user can effectively improve the coverage probability of a cell center macro-user, and hence improve the overall coverage probability. Fig. 7 plots the coverage probability versus the maximum IN DoF in the high SIR threshold regime. From Fig. 7, we can see that $U^*(\beta, T_1, T_2) = 0$. This verifies *Lemma 5*. In addition, we can observe that the coverage probability decreases with the maximum IN DoF.

VII. Numerical Experiments

In this section, we compare the proposed user-centric IN scheme with two baseline schemes. One is the simple beamforming scheme (without interference management), which can be treated as a special case of our IN scheme by setting $U = 0$ and/or $T_1 = T_2 = 1$. The other is a modified version of the existing ABS scheme in 3GPP-LTE, referred to as the user-centric ABS scheme. The user-centric ABS scheme has three design parameters, i.e., a resource partition parameter η and two thresholds T_1 and T_2, where T_j ($j = 1, 2$) is the threshold for the j-th tier. We define a potential ABS macro-BS of a scheduled user in a similar way to a potential IN macro-BS of a scheduled user in the user-centric IN scheme. In each slot, each scheduled user sends ABS requests to all of its potential ABS macro-BSs. We define the potential ABS users of a macro-BS in a similar way to the potential IN users of a marco-BS in the user-centric IN scheme. $1 - \eta$ fraction of (time or frequency) resource is allocated to all the potential ABS macro-BSs to serve their scheduled users, while η fraction of resource is allocated to the remaining BSs to serve their own scheduled users.[14] Then, for given T_1 and T_2, we choose the optimal η to maximize the coverage probability of the user-centric IN scheme.

Note that the benefit of the proposed user-centric IN scheme compared to the simple beamforming scheme is that it can optimally allocate DoF in boosting desired signals and managing interference. Thus, the performance of the proposed user-centric IN scheme is always better than

[14]Under this user-centric ABS scheme, each scheduled potential ABS pico-user or macro-user whose serving macro-BS is not a potential ABS macro-BS can avoid the interference from all its potential ABS macro-BSs via resource partition in ABS.

that of the simple beamforming scheme. The benefit of the proposed user-centric IN scheme compared to the user-centric ABS is that it does not have (time or frequency) resource sacrifice. On the other hand, one loss of the proposed user-centric IN scheme compared to the user-centric ABS is due to the DoF reduction for boosting desired signals to macro-users. The other loss of the proposed user-centric IN scheme compared to the user-centric ABS is caused by the remaining macro-interference, as the IN scheme only avoids the strong macro-interference to the potential IN users, while ABS avoids all the macro interference to the potential ABS users.

Fig. 7 illustrates the coverage probability versus the number of antennas at each macro-BS N_1. From Fig. 7, we can observe that the proposed user-centric IN scheme and the user-centric ABS outperform the simple beamforming scheme, demonstrating the importance of interference management in the parameter region considered in this figure. In addition, the proposed user-centric IN scheme outperforms the user-centric ABS when N_1 is relatively large. The reason is as follows. When N_1 is relatively large, for serving macro-users, the loss of the user-centric ABS caused by (time or frequency) resource sacrifice (due to resource partition) is large, while the loss of the proposed user-centric IN scheme caused by the DoF reduction (due to performing IN) is small. Fig. 8 illustrates the coverage probability versus the path loss exponent in the marco-cell tier α_1. From Fig. 8, we can observe that the proposed user-centric IN scheme outperforms the user-centric ABS when α_1 is relatively large. The reason is as follows. When α_1 is large, the loss of the user-centric ABS caused by (time or frequency) resource sacrifice is large, while the loss of the proposed user-centric IN scheme due to the remaining macro-interference is small.[15]

VIII. Conclusions

In this paper, we proposed a user-centric IN scheme in downlink two-tier multi-antenna HetNets. Using tools from stochastic geometry, we first obtained a tractable expression of the coverage probability. Then, we obtained the asymptotic expressions of the outage and coverage probabilities in the low and high SIR threshold regimes, respectively. The asymptotic expressions indicate that the maximum IN DoF and the IN thresholds affect the asymptotic outage (coverage) probability in dramatically different ways. Moreover, we characterized the optimal maximum IN

[15]The observation that the proposed scheme outperforms ABS when N_1 or α_1 is relatively large is similar to the observation made in [14]. The reason can be found in Footnote 11.

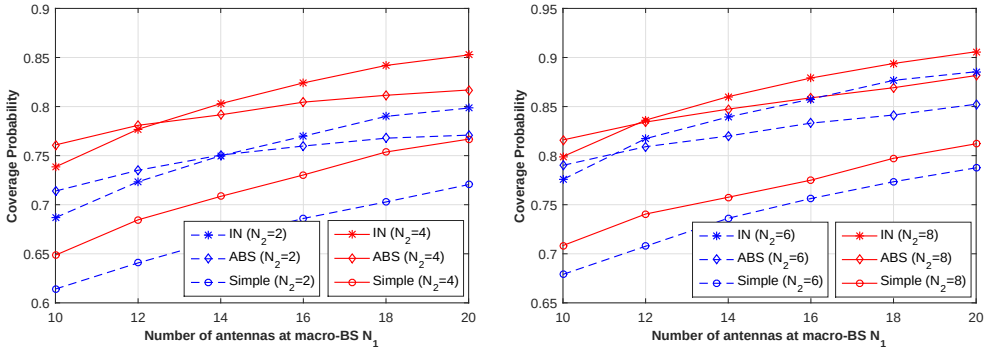

(a) $N_2 = 2$ and $N_2 = 4$ (b) $N_2 = 6$ and $N_2 = 8$

Fig. 7. Coverage probability versus number of antennas at each macro-BS. $\alpha_1 = \alpha_2 = 4.5$, $T_1 = T_2 = 6$ $\frac{P_1}{P_2} = 15$ dB, $\lambda_1 = 0.0005$ nodes/m^2, and $\lambda_2 = 0.001$ nodes/m^2.

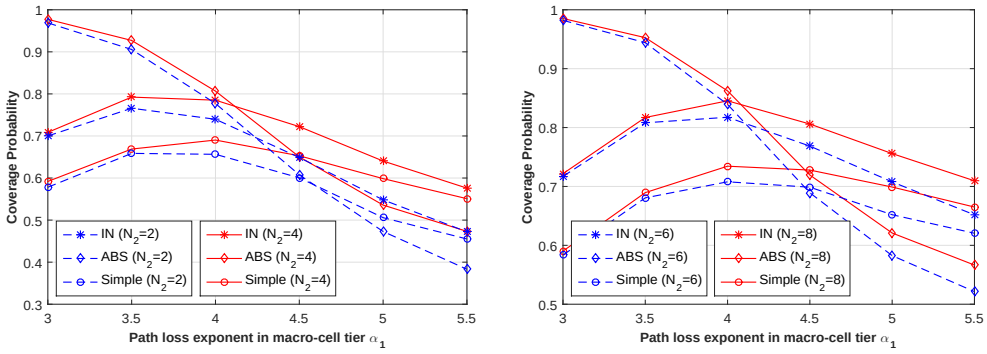

(a) $N_2 = 2$ and $N_2 = 4$ (b) $N_2 = 6$ and $N_2 = 8$

Fig. 8. Coverage probability versus path loss exponent in marco-cell tier. $N_1 = 16$, $\alpha_2 = 4$, $T_1 = T_2 = 6$, $\frac{P_1}{P_2} = 15$ dB, $\lambda_1 = 0.0005$ nodes/m^2, and $\lambda_2 = 0.001$ nodes/m^2.

DoF which optimizes the outage (coverage) probability. The optimization results reveal that the IN scheme can linearly improve the performance in the low SIR threshold regime, but cannot improve the performance in the high SIR threshold regime. Finally, numerical results showed that the user-centric IN scheme can achieve good performance gains over existing schemes.

APPENDIX

A. *Proof of Lemma 1*

According to Slivnyak's theorem [24], we focus on a macro-BS located at origin, referred to as macro-BS 0. Note that both scheduled macro-users and scheduled pico-users may send IN requests to macro-BS 0. We first characterize the probability that a scheduled macro-user sends an IN request to macro-BS 0. Denote R_{1i} as the distance between macro-BS 0 and a

randomly selected (according to the uniform distribution) scheduled macro-user, referred to as scheduled macro-user i. Hence, Scheduled macro-user i sends an IN request to macro-BS 0 with probability $p_{1i}(T_1) = \Pr\left(T_1^{-\frac{1}{\alpha_1}} R_{1i} < Y_1 < R_{1i}\right)$. Assume that the scheduled macro-users form a homogeneous PPP with density λ_1. Conditioned on $R_{1i} = r$, we have

$$p_{1i,R_{1i}}(r, T_1) = \Pr\left(T_1^{-\frac{1}{\alpha_1}} r < Y_1 < r\right) = \int_{T_1^{-\frac{1}{\alpha_1}} r}^{r} f_{Y_1}(y)\mathrm{d}y \tag{28}$$

where $f_{Y_1}(y)$ is the probability density function (p.d.f.) of Y_1 given by (7). Then, the scheduled macro-user density at distance r away from macro-BS 0 is $p_{1i,R_{1i}}(r, T_1)\lambda_1$. This indicates that the scheduled macro-users at distance r away from macro-BS 0 which send IN requests to macro-BS 0 form an inhomogeneous PPP with density $p_{1i,R_{1i}}(r, T_1)\lambda_1$. Next, we characterize the probability that a scheduled pico-user sends an IN request to macro-BS 0. Denote R_{2i} as the distance between macro-BS 0 and a randomly selected (according to the uniform distribution) scheduled pico-user, referred to as scheduled pico-user i. Similarly, we assume that the scheduled pico-users form a homogeneous PPP with density λ_2, and it is independent of the PPP formed by the scheduled macro-users. Then, we can show that the scheduled pico-users at distance r away from macro-BS 0 which send IN requests to macro-BS 0 form an inhomogeneous PPP with density $p_{2i,R_{2i}}(r, T_2)\lambda_2$, where

$$p_{2i,R_{2i}}(r, T_2) = \Pr\left(\left(\frac{P_2}{P_1 T_2}\right)^{\frac{1}{\alpha_2}} r^{\frac{\alpha_1}{\alpha_2}} < Y_2 < \left(\frac{P_2}{P_1}\right)^{\frac{1}{\alpha_2}} r^{\frac{\alpha_1}{\alpha_2}}\right) = \int_{\left(\frac{P_2}{P_1 T_2}\right)^{\frac{1}{\alpha_2}} r^{\frac{\alpha_1}{\alpha_2}}}^{\left(\frac{P_2}{P_1}\right)^{\frac{1}{\alpha_2}} r^{\frac{\alpha_1}{\alpha_2}}} f_{Y_2}(y)\mathrm{d}y. \tag{29}$$

Note that $f_{Y_2}(y)$ is the p.d.f. of Y_2 given by (8).

According to the superposition property of PPPs [24], the scheduled macro-users and the scheduled pico-users at distance r away from macro-BS 0 which send IN requests to macro-BS 0, i.e., the potential IN users of macro-BS 0, still form a PPP with density $p_{1i,R_{1i}}(r, T_1)\lambda_1 + p_{2i,R_{2i}}(r, T_2)\lambda_2$. Therefore, the number of the potential IN users of macro-BS 0 is Poisson distributed with parameter (i.e., mean) $\bar{L}(T_1, T_2) = 2\pi \int_0^\infty r \left(p_{1i,R_{1i}}(r, T_1)\lambda_1 + p_{2i,R_{2i}}(r, T_2)\lambda_2\right) \mathrm{d}r = \bar{L}_1(T_1) + \bar{L}_2(T_2)$.

B. Proof of Lemma 3

From Section III-A, we know that whether a scheduled user sends an IN request to a macro-BS or not depends on its location relative to this macro-BS. Hence, the event that u_0 sends an IN request to one of its potential IN macro-BSs and the event that any other scheduled user sends an IN request to the same macro-BS are dependent. For analytical tractability, we approximate

TABLE I

PARAMETER VALUES

j	$R_{j,1C}$	$R_{j,1O}$	$R_{j,2}$
1	Y_1	$T_1^{\frac{1}{\alpha_1}} Y_1$	$\left(\frac{P_2}{P_1}\right)^{\frac{1}{\alpha_2}} Y_1^{\frac{\alpha_1}{\alpha_2}}$
2	$\left(\frac{P_1}{P_2}\right)^{\frac{1}{\alpha_1}} Y_2^{\frac{\alpha_2}{\alpha_1}}$	$\left(\frac{P_1}{P_2}T_2\right)^{\frac{1}{\alpha_1}} Y_2^{\frac{\alpha_2}{\alpha_1}}$	Y_2

these two events as independent events. Then, we have

$$p_c\left(U,T_1,T_2\right) \approx \mathrm{E}\left[\min\left\{\frac{U}{K_0+1},1\right\}\right] = \sum_{k=0}^{U-1}\Pr\left(K_0=k\right) + \sum_{k=U}^{\infty}\frac{U}{k+1}\Pr\left(K_0=k\right)\ . \tag{30}$$

Substituting (5) into (30), we have the final result.

C. Proof of Theorem 1

Let $R_{j,1C}$ and $R_{j,1O}$ denote the minimum and maximum possible distances between $u_0 \in \mathcal{U}_j$ and its nearest and furthest macro-interferers (among u_0's potential IN macro-BSs which do not select u_0 for IN), respectively. Let $R_{j,2}$ denote the minimum possible distance between $u_0 \in \mathcal{U}_2$ and its nearest pico-interferer. The relationships between $R_{j,1C}$, $R_{j,1O}$, $R_{j,2}$, and Y_j, respectively, are shown in Table I. Based on (4) and conditioned on $Y_j = y$, we have

$$\begin{aligned}
&\Pr\left(\mathrm{SIR}_0 > \beta | u_0 \in \mathcal{U}_j, Y_j = y\right)\\
=&\Pr\left(\left|\mathbf{h}_{j,00}^{\dagger}\mathbf{f}_{j,0}\right|^2 > \beta y^{\alpha_j}\left(\frac{P_1}{P_j}I_{j,1C} + \frac{P_1}{P_j}I_{j,1O} + \frac{P_2}{P_j}I_{j,2}\right)\right)\\
=&\sum_{n=0}^{M_j-1}\frac{\left(\beta y^{\alpha_j}\right)^n}{n!}\sum_{\left(n_a\right)_{a=1}^3\in\mathcal{N}_n}\binom{n}{n_1,n_2,n_3}\left(\frac{P_1}{P_j}\right)^{n_1+n_2}\left(\frac{P_2}{P_j}\right)^{n_3}\mathrm{E}_{I_{j,1C}}\left[I_{j,1C}^{n_1}\exp\left(-\beta y^{\alpha_j}\frac{P_1}{P_j}I_{j,1C}\right)\right]\\
&\times\mathrm{E}_{I_{j,1O}}\left[I_{j,1O}^{n_2}\exp\left(-\beta y^{\alpha_j}\frac{P_1}{P_j}I_{j,1O}\right)\right]\mathrm{E}_{I_{j,2}}\left[I_{j,2}^{n_3}\exp\left(-\beta y^{\alpha_j}\frac{P_2}{P_j}I_{j,2}\right)\right]\\
=&\sum_{n=0}^{M_j-1}\frac{\left(-\beta y^{\alpha_j}\right)^n}{n!}\sum_{\left(n_a\right)_{a=1}^3\in\mathcal{N}_n}\binom{n}{n_1,n_2,n_3}\left(\frac{P_1}{P_j}\right)^{n_1+n_2}\left(\frac{P_2}{P_j}\right)^{n_3}\mathcal{L}_{I_{j,1C}}^{(n_1)}\left(U,s,r_{j,1C},r_{j,1O}\right)|_{s=\beta y^{\alpha_j}\frac{P_1}{P_j}}\\
&\times\mathcal{L}_{I_{j,1O}}^{(n_2)}\left(s,r_{j,1O}\right)|_{s=\beta y^{\alpha_j}\frac{P_1}{P_j}}\mathcal{L}_{I_{j,2}}^{(n_3)}(s,r_{j,2})|_{s=\beta y^{\alpha_j}\frac{P_2}{P_j}}
\end{aligned} \tag{31}$$

where $\mathcal{L}_I^{(n)}(s,r)$ denotes the nth-order derivative of the Laplace transform $\mathcal{L}_I(s,r)$.

Now, we calculate $\mathcal{L}_I(s,r)$ and $\mathcal{L}_I^{(n)}(s,r)$, respectively. First, $\mathcal{L}_{I_{j,1C}}(U,s,r_{j,1C},r_{j,1O})$ can be

calculated as follows:

$$\begin{aligned}\mathcal{L}_{I_{j,1C}}(U,s,r_{j,1C},r_{j,1O}) &= \mathrm{E}_{\Phi_{j,1C},\{\mathbf{g}_{1,\ell}\}}\left[\exp(-s\sum_{\ell\in\Phi_{j,1C}} D_{1,\ell 0}^{-\alpha_1}\mathbf{g}_{1,\ell}\right] \\ &\overset{(a)}{=} \mathrm{E}_{\Phi_{j,1C}}\left[\prod_{\ell\in\Phi_{j,1C}} \mathrm{E}_{\{\mathbf{g}_{1,\ell}\}}\left[\exp(-sD_{1,\ell 0}^{-\alpha_1}\mathbf{g}_{1,\ell}\right]\right] = \mathrm{E}_{\Phi_{j,1C}}\left[\prod_{\ell\in\Phi_{j,1C}} \frac{1}{1+sD_{1,\ell 0}^{-\alpha_1}}\right] \\ &\overset{(b)}{=} \exp\left(-2\pi p_{\bar{c}}\left(U,T_1,T_2\right)\lambda_1\int_{r_{j,1C}}^{r_{j,1O}}\left(1-\frac{1}{1+\frac{s}{r^{\alpha_1}}}\right)r\mathrm{d}r\right) \end{aligned} \tag{32}$$

where $\mathbf{g}_{1,\ell}=\left|\mathbf{h}_{1,\ell 0}^{\dagger}\mathbf{f}_{1,\ell}\right|^2$, (a) is obtained by noting that $\mathbf{g}_{1,\ell}$ ($\ell\in\Phi_{j,1C}$) are mutually independent, and (b) is obtained by using the probability generating functional of a PPP [24]. Further, by first letting $s^{-\frac{1}{\alpha_1}}r=t$ and then $\frac{1}{1+t^{-\alpha_1}}=w$, we obtain the result in (15).

Next, based on (32) and utilizing Faà di Bruno's formula [25], $\mathcal{L}_{I_{j,1C}}^{(n_1)}(U,s,r_{j,1C},r_{j,1O})$ can be calculated as follows:

$$\begin{aligned}\mathcal{L}_{I_{j,1C}}^{(n_1)}(U,s,r_{j,1C},r_{j,1O}) =& \mathcal{L}_{I_{j,1C}}(U,s,r_{j,1C},r_{j,1O})\sum_{(m_a)_{a=1}^{n}\in\mathcal{M}_{n_1}}\frac{n_1!}{\prod_{a=1}^{n_1}(a!)^{m_a}m_a!} \\ &\times\prod_{a=1}^{n_1}\left(2\pi p_{\bar{c}}\left(U,T_1,T_2\right)\lambda_1\int_{r_{j,1C}}^{r_{j,1O}}\frac{\mathrm{d}^a}{\mathrm{d}s^a}\left(\frac{1}{1+\frac{s}{r^{\alpha_1}}}\right)r\mathrm{d}r\right)^{m_a} \\ =& \mathcal{L}_{I_{j,1C}}(U,s,r_{j,1C},r_{j,1O})\sum_{(m_a)_{a=1}^{n}\in\mathcal{M}_{n_1}}\frac{n_1!(-1)^{n_1}}{\prod_{a=1}^{n_1}(a!)^{m_a}m_a!} \\ &\times\prod_{a=1}^{n_1}\left(2\pi p_{\bar{c}}\left(U,T_1,T_2\right)\lambda_1\Gamma\left(a+1\right)\int_{r_{j,1C}}^{r_{j,1O}}\frac{r^{1-a\alpha_1}}{\left(1+\frac{s}{r^{\alpha_1}}\right)^{a+1}}\mathrm{d}r\right)^{m_a}\end{aligned} \tag{33}$$

where the integral can be solved using a similar method. Similarly, we can calculate $\mathcal{L}_{I_{j,1O}}(s,r_{j,1O})$, $\mathcal{L}_{I_{j,1O}}^{(n_2)}(s,r_{j,1O})$, $\mathcal{L}_{I_{j,2}}(s,r_{j,2})$ and $\mathcal{L}_{I_{j,2}}^{(n_3)}(s,r_{j,2})$. Finally, removing the conditions on $Y_j=y$ and after some algebraic manipulations, we can obtain the final result.

D. Proof of Theorem 2

Conditioned on $Y_j=y$, we have

$$\begin{aligned}&1-\Pr\left(\mathrm{SIR}_0>\beta|u_0\in\mathcal{U}_j,Y_j=y\right) \\ =&\Pr\left(\left|\mathbf{h}_{j,00}^{\dagger}\mathbf{f}_{j,0}\right|^2\le\beta y^{\alpha_j}\left(\frac{P_1}{P_j}I_{j,1C}+\frac{P_1}{P_j}I_{j,1O}+\frac{P_2}{P_j}I_{j,2}\right)\right) \\ =&\exp\left(-\beta y^{\alpha_j}\left(\frac{P_1}{P_j}I_{j,1C}+\frac{P_1}{P_j}I_{j,1O}+\frac{P_2}{P_j}I_{j,2}\right)\right)\sum_{n=M_j}^{\infty}\frac{(\beta y^{\alpha_j})^n}{n!}\left(\frac{P_1}{P_j}I_{j,1C}+\frac{P_1}{P_j}I_{j,1O}+\frac{P_2}{P_j}I_{j,2}\right)^n\end{aligned}$$

$$= \sum_{n=M_j}^{\infty} \frac{(-\beta y^{\alpha_j})^n}{n!} \sum_{(n_a)_{a=1}^3 \in \mathcal{N}_n} \binom{n}{n_1, n_2, n_3} \left(\frac{P_1}{P_j}\right)^{n_1+n_2} \mathcal{L}_{I_{j,1C}}^{(n_1)} \left(U, s, r_{j,1C}, r_{j,1O}\right)|_{s=\beta y^{\alpha_j}\frac{P_1}{P_j}}$$

$$\times \mathcal{L}_{I_{j,1O}}^{(n_2)} \left(s, r_{j,1O}\right)|_{s=\beta y^{\alpha_j}\frac{P_1}{P_j}} \left(\frac{P_2}{P_j}\right)^{n_3} \mathcal{L}_{I_{j,2}}^{(n_3)}(s, r_{j,2})|_{s=\beta y^{\alpha_j}\frac{P_2}{P_j}} . \tag{34}$$

Similar to the calculations in Appendix C, after some algebraic manipulations and removing the condition on $Y_j = y$, we have

$$1 - \mathcal{S}_j\left(U, T_1, T_2, \beta\right) = \int_0^{\infty} \sum_{n=M_j}^{\infty} \mathcal{T}_{j,Y_j}\left(n, y, U, T_1, T_2, \beta\right) f_{Y_j}(y)\mathrm{d}y \tag{35}$$

where

$$\mathcal{T}_{j,Y_j}\left(n, y, U, T_1, T_2, \beta\right) = \frac{1}{n!} \sum_{(n_a)_{a=1}^3 \in \mathcal{N}_n} \binom{n}{n_1, n_2, n_3} \tilde{\mathcal{L}}_{I_{j,1C}}^{(n_1)}\left(U, s, y\right)|_{s=\beta y^{\alpha_j}\frac{P_1}{P_j}} \tilde{\mathcal{L}}_{I_{j,1O}}^{(n_2)}\left(s, y\right)|_{s=\beta y^{\alpha_h}\frac{P_1}{P_j}}$$

$$\times \tilde{\mathcal{L}}_{I_{j,2}}^{(n_3)}\left(s, y\right)|_{s=\beta y^{\alpha_j}\frac{P_2}{P_j}} . \tag{36}$$

Now, we calculate $\lim_{\beta\to 0} \int_0^{\infty} \sum_{n=M_j}^{\infty} \mathcal{T}_{j,Y_j}\left(n, y, U, T_1, T_2, \beta\right) f_{Y_j}(y)\mathrm{d}y$, i.e., the asymptotic outage probability when $\beta \to 0$. We note that $B^{'}(a, b, z) = \frac{(1-z)^b}{b} + o\left((1-z)^b\right)$ as $z \to 1$. Then, we have

$$B^{'}\left(\frac{2}{\alpha}, 1 - \frac{2}{\alpha}, \frac{1}{1+c\beta}\right) = \frac{(c\beta)^{1-\frac{2}{\alpha}}}{1-\frac{2}{\alpha}} + o\left(\beta^{1-\frac{2}{\alpha}}\right) , \tag{37}$$

$$B^{'}\left(1 + \frac{2}{\alpha}, a - \frac{2}{\alpha}, \frac{1}{1+c\beta}\right) = \frac{(c\beta)^{a-\frac{2}{\alpha}}}{a-\frac{2}{\alpha}} + o\left(\beta^{a-\frac{2}{\alpha}}\right) , \tag{38}$$

where $c \in \mathbb{R}^+$. Based on these two asymptotic expressions, we can obtain[16]

$$\tilde{\mathcal{L}}_{I_{j,1C}}^{(n_1)}\left(U, s, y\right) = \beta^{n_1} \sum_{(m_a)_{a=1}^{n_1} \in \mathcal{M}_{n_1}} \frac{n_1!}{\prod_{a=1}^{n_1} m_a!} \prod_{a=1}^{n_1} \left(\frac{\frac{2\pi}{\alpha_1} p_{\bar{c}}\left(U, T_1, T_2\right)\lambda_1}{a-\frac{2}{\alpha_1}} \left(1 - \left(\frac{1}{T_j}\right)^{a-\frac{2}{\alpha_1}}\right) \left(\frac{P_1 y^{\alpha_j}}{P_j}\right)^{\frac{2}{\alpha_1}}\right)^{m_a} + o\left(\beta^{n_1}\right) , \tag{39}$$

$$\tilde{\mathcal{L}}_{I_{j,1O}}^{(n_2)}\left(s, y\right) = \beta^{n_2} \sum_{(p_a)_{a=1}^{n_2} \in \mathcal{M}_{n_2}} \frac{n_2!}{\prod_{a=1}^{n_2} p_a!} \prod_{a=1}^{n_2} \left(\frac{\frac{2\pi}{\alpha_1}\lambda_1}{a-\frac{2}{\alpha_1}} \left(\frac{P_1}{P_j}\right)^{\frac{2}{\alpha_1}} y^{\frac{2\alpha_j}{\alpha_1}} \left(\frac{1}{T_j}\right)^{a-\frac{2}{\alpha_1}}\right)^{p_a} + o\left(\beta^{n_2}\right) , \tag{40}$$

$$\tilde{\mathcal{L}}_{I_{j,2}}^{(n_3)}\left(s, y\right) = \beta^{n_3} \sum_{(q_a)_{a=1}^{n_3} \in \mathcal{M}_{n_3}} \frac{n_3!}{\prod_{a=1}^{n_2} q_a!} \prod_{a=1}^{n_3} \left(\frac{\frac{2\pi}{\alpha_2}\lambda_2}{a-\frac{2}{\alpha_2}} \left(\frac{P_2}{P_j}\right)^{\frac{2}{\alpha_2}} y^{\frac{2\alpha_j}{\alpha_2}}\right)^{q_a} + o\left(\beta^{n_3}\right) . \tag{41}$$

Moreover, utilizing dominated convergence theorem, we can show that

$$\lim_{\beta\to 0} \int_0^{\infty} \sum_{n=M_j}^{\infty} \mathcal{T}_{j,Y_j}\left(n, y, U, T_1, T_2, \beta\right) f_{Y_j}(y)\mathrm{d}y = \int_0^{\infty} \sum_{n=M_j}^{\infty} \lim_{\beta\to 0} \mathcal{T}_{j,Y_j}\left(n, y, U, T_1, T_2, \beta\right) f_{Y_j}(y)\mathrm{d}y .$$

Hence, substituting (39), (40) and (41) into (35), and after some algebraic manipulations, we obtain Results 1), 2) and 3) in *Theorem 2*. To complete the proof, we now show that $b_2\left(U, T_1, T_2\right)$ decreases with U. This can be proved by noting that i) $b_2\left(U, T_1, T_2\right)$ is an increasing function of $p_{\bar{c}}\left(U, T_1, T_2\right)$, and ii) $p_{\bar{c}}\left(U, T_1, T_2\right)$ decreases with U (which can be easily shown using (30)).

[16] $f(x) = o\left(g(x)\right)$ means $\lim_{x\to 0} \frac{f(x)}{g(x)} = 0$.

E. Proof of Lemma 4

First, we characterize the maximum order gain. When $U \in \{0,1,\ldots,N_1-N_2\}$, we have $N_1-U \geq N_2$, implying $\min\{N_1-U,N_2\}=N_2$. When $U \in \{N_1-N_2+1,\ldots,N_1-1\}$, we have $N_1-U<N_2$, implying $\min\{N_1-U,N_2\}=N_1-U<N_2$. Thus, we can show that the maximum order gain is $\max_{U\in\{0,1,\cdots,N_1-1\}}\min\{N_1-U,N_2\}=N_2$, achieved at $U\in\{0,1,\ldots,N_1-N_2\}$. Next, we compare the coefficients of β^{N_2} achieved at different $U\in\{0,1,\ldots,N_1-N_2\}$. We consider two cases. i) When $U<N_1-N_2$, as $b_2\left(U,T_1,T_2\right)$ decreases with U, the coefficients satisfy $b_2\left(N_1-N_2-1,T_1,T_2\right) < b_2\left(N_1-N_2-2,T_1,T_2\right) < \ldots < b_2\left(0,T_1,T_2\right)$. ii) When $U=N_1-N_2$, the coefficient of β^{N_2} is $b_1\left(N_1-N_2,T_1,T_2\right)+b_2\left(N_1-N_2,T_1,T_2\right)$. Therefore, we can complete the proof.

F. Proof of Theorem 3

1) Upper Bound: Let $\mathcal{S}_{j,Y_j}\left(y,\beta,U,T_1,T_2\right)\triangleq \Pr\left(\mathrm{SIR}_0>\beta|u_0\in\mathcal{U}_j,Y_j=y\right)$ denote the conditional SIR coverage probability. Then, $\mathcal{S}_j\left(\beta,U,T_1,T_2\right)$ can be written as

$$\mathcal{S}_j\left(\beta,U,T_1,T_2\right)=\int_0^\infty \mathcal{S}_{j,Y_j}\left(y,\beta,U,T_1,T_2\right)f_{Y_j}(y)\mathrm{d}y \tag{42}$$

where $\mathcal{S}_{j,Y_j}\left(y,\beta,U,T_1,T_2\right)=\mu_j\left(\beta,U,T_1,T_2\right)g_j\left(y,\beta,U,T_1,T_2\right)$ and $f_{Y_j}(y)$ is the p.d.f. of Y_j given in *Lemma 1*. Here, $g_j\left(y,\beta,U,T_1,T_2\right)=\exp\left(-c_1\beta^{\frac{2}{\alpha_1}}y^{\frac{2\alpha_j}{\alpha_1}}-c_2\beta^{\frac{2}{\alpha_2}}y^{\frac{2\alpha_j}{\alpha_2}}\right)$ with $c_1=\left(p_{\bar{c}}\left(U,T_1,T_2\right)\left(B'\left(\frac{2}{\alpha_1},1-\frac{2}{\alpha_1},\frac{1}{1+\beta}\right)-B'\left(\frac{2}{\alpha_1},1-\frac{2}{\alpha_1},\frac{1}{1+\frac{\beta}{T_j}}\right)\right)+B'\left(\frac{2}{\alpha_1},1-\frac{2}{\alpha_1},\frac{1}{1+\frac{\beta}{T_j}}\right)\right)\times\frac{2\pi\lambda_1}{\alpha_1}\left(\frac{P_1}{P_j}\right)^{\frac{2}{\alpha_1}}$ and $c_2=\frac{2\pi\lambda_2}{\alpha_2}\left(\frac{P_2}{P_j}\right)^{\frac{2}{\alpha_2}}B'\left(\frac{2}{\alpha_2},1-\frac{2}{\alpha_2},\frac{1}{1+\beta}\right)$, and $\mu_j\left(\beta,U,T_1,T_2\right)=c(\beta)\times y^{\frac{2\alpha_j}{\alpha_1}\left(\sum_{a=1}^{n_1}m_a+\sum_{a=1}^{n_2}p_a\right)+\frac{2\alpha_j}{\alpha_2}\sum_{a=1}^{n_3}q_a}$, where

$$\begin{aligned}c(\beta)=&\sum_{n=0}^{M_j-1}\frac{1}{n!}\sum_{(n_a)_{a=1}^3\in\mathcal{N}_n}\sum_{(m_a)_{a=1}^{n_1}\in\mathcal{M}_{n_1}}\sum_{(p_a)_{a=1}^{n_2}\in\mathcal{M}_{n_2}}\sum_{(q_a)_{a=1}^{n_3}\in\mathcal{M}_{n_3}}\binom{n}{n_1,n_2,n_3}\frac{n_1!}{\prod_{a=1}^{n_1}m_a!}\\
&\times\prod_{a=1}^{n_1}\left(\frac{2\pi\lambda_1}{\alpha_1}p_{\bar{c}}\left(U,T_1,T_2\right)\left(\frac{\beta P_1}{P_j}\right)^{\frac{2}{\alpha_1}}\right)^{m_a}\prod_{a=1}^{n_2}\left(\frac{2\pi\lambda_1}{\alpha_1}\left(\frac{\beta P_1}{P_j}\right)^{\frac{2}{\alpha_1}}B'\left(1+\frac{2}{\alpha_1},a-\frac{2}{\alpha_1},\frac{1}{1+\frac{\beta}{T_j}}\right)\right)^{p_a}\\
&\times\prod_{a=1}^{n_1}\left(B'\left(1+\frac{2}{\alpha_1},a-\frac{2}{\alpha_1},\frac{1}{1+\beta}\right)-B'\left(1+\frac{2}{\alpha_1},a-\frac{2}{\alpha_1},\frac{1}{1+\frac{\beta}{T_j}}\right)\right)^{m_a}\frac{n_2!}{\prod_{a=1}^{n_2}p_a!}\frac{n_3!}{\prod_{a=1}^{n_3}q_a!}\\
&\times\prod_{a=1}^{n_3}\left(\frac{2\pi\lambda_2}{\alpha_2}\left(\frac{\beta P_2}{P_j}\right)^{\frac{2}{\alpha_2}}B'\left(1+\frac{2}{\alpha_2},a-\frac{2}{\alpha_2},\frac{1}{1+\beta}\right)\right)^{q_a}.\end{aligned} \tag{43}$$

Let $\tilde{\mathcal{S}}_{j,Y_j}\left(y,\beta,U,T_1,T_2\right)=\mu_j\left(\beta,U,T_1,T_2\right)\tilde{g}_j\left(y,\beta,U,T_1,T_2\right)$ with $\tilde{g}_j\left(y,\beta,U,T_1,T_2\right)=\exp\left(-c_j\beta^{\frac{2}{\alpha_j}}y^2\right)$. Let $\tilde{f}_{Y_j}(y)=\frac{2\pi\lambda_j}{\mathcal{A}_j}y\exp\left(-a_1y^2\right)$. Then, we have

$$\begin{aligned}&\int_0^\infty \mathcal{S}_{j,Y_j}\left(y,\beta,U,T_1,T_2\right)f_{Y_j}(y)\mathrm{d}y<\int_0^\infty \tilde{\mathcal{S}}_{j,Y_j}\left(y,\beta,U,T_1,T_2\right)\tilde{f}_{Y_j}(y)\mathrm{d}y\\&=\frac{c(\beta)\pi\lambda_j}{\mathcal{A}_j}\left(c_j\beta^{\frac{2}{\alpha_j}}+a_1\right)^{-\frac{\alpha_j}{\alpha_1}\left(\sum_{a=1}^{n_1}m_a+\sum_{a=1}^{n_2}p_a\right)-\frac{\alpha_j}{\alpha_2}\sum_{a=1}^{n_3}q_a-1}\\&\quad\times\Gamma\left(\frac{\alpha_j}{\alpha_1}\left(\sum_{a=1}^{n_1}m_a+\sum_{a=1}^{n_2}p_a\right)+\frac{\alpha_j}{\alpha_2}\sum_{a=1}^{n_3}q_a+1\right).\end{aligned}\tag{44}$$

Based on (38), we can obtain the order of β as $\beta\to\infty$: $\beta^{-\left(1+\frac{2}{\alpha_1}\right)\sum_{a=1}^{n_1}m_a-\frac{2}{\alpha_j}}$, which can be maximized when $n_1=0$. Hence, we obtain the order of the upper bound: $\beta^{-\frac{2}{\alpha_j}}$. Moreover, based on (37) and after some algebraic manipulation, we obtain the expression of $\eta_1(U,T_1,T_2)$ and η_2.

2) Lower Bound: First, we note that $\mathcal{S}_j\left(\beta,U,T_1,T_2\right)$ can be rewritten as

$$\begin{aligned}&\mathcal{S}_j\left(\beta,U,T_1,T_2\right)=\int_0^1\mathcal{S}_{j,Y_j}\left(y,\beta,U,T_1,T_2\right)f_{Y_j}(y)\mathrm{d}y+\int_1^\infty\mathcal{S}_{j,Y_j}\left(y,\beta,U,T_1,T_2\right)f_{Y_j}(y)\mathrm{d}y\\&>\int_0^1\mathcal{S}_{j,Y_j}\left(y,\beta,U,T_1,T_2\right)f_{Y_j}(y)\mathrm{d}y>\int_0^1\hat{\mathcal{S}}_{j,Y_j}\left(y,\beta,U,T_1,T_2\right)\hat{f}_{Y_j}(y)\mathrm{d}y\\&=c(\beta)\frac{\pi\lambda_j}{\mathcal{A}_j}\frac{\alpha_{\max}}{\alpha_j}\left(a_1+a_2+c_1\beta^{\frac{2}{\alpha_1}}+c_2\beta^{\frac{2}{\alpha_2}}\right)^{-\frac{\alpha_{\max}}{\alpha_1}\left(\sum_{a=1}^{n_1}m_a+\sum_{a=1}^{n_2}p_a\right)-\frac{\alpha_{\max}}{\alpha_2}\sum_{a=1}^{n_3}q_a-\frac{\alpha_{\max}}{\alpha_j}}\\&\times\gamma\left(\frac{\alpha_{\max}}{\alpha_1}\left(\sum_{a=1}^{n_1}m_a+\sum_{a=1}^{n_2}p_a\right)+\frac{\alpha_{\max}}{\alpha_2}\sum_{a=1}^{n_3}q_a+\frac{\alpha_{\max}}{\alpha_j},a_1+a_2+c_1\beta^{\frac{2}{\alpha_1}}+c_2\beta^{\frac{2}{\alpha_2}}\right)\end{aligned}\tag{45}$$

where $\hat{\mathcal{S}}_{j,Y_j}\left(y,\beta,U,T_1,T_2\right)=\mu_j(\beta,U,T_1,T_2)\hat{g}_j(y,\beta,U,T_1,T_2)$ with $\hat{g}_j(y,\beta,U,T_1,T_2)$ $=\exp\left(-c_1\beta^{\frac{2}{\alpha_1}}y^{\frac{2\alpha_j}{\alpha_{\max}}}-c_2\beta^{\frac{2}{\alpha_2}}y^{\frac{2\alpha_j}{\alpha_{\max}}}\right)$, and $\hat{f}_{Y_j}(y)=\frac{2\pi\lambda_j}{\mathcal{A}_j}y\exp\left(-a_1y^{\frac{2\alpha_j}{\alpha_{\max}}}-a_2y^{\frac{2\alpha_j}{\alpha_{\max}}}\right)$. Similar to the method in calculating the order of the upper bound, when $\beta\to\infty$, we can obtain the order of the lower bound as $\beta^{-\sum_{a=1}^{n_1}m_a+\frac{2}{\alpha_1}\sum_{a=1}^{n_2}p_a+\frac{2}{\alpha_2}\sum_{a=1}^{n_3}q_a-\frac{2\alpha_{\max}}{\alpha_{\min}\alpha_1}\left(\sum_{a=1}^{n_1}m_a+\sum_{a=1}^{n_2}p_a\right)-\frac{2\alpha_{\max}}{\alpha_{\min}\alpha_2}\sum_{a=1}^{n_3}q_a-\frac{2}{\alpha_j}\frac{\alpha_{\max}}{\alpha_j}}$, which can be maximized when $n_1=n_2=n_3=0$, i.e., $n=0$. Hence, we obtain the order of the lower bound as $\beta^{-\frac{2}{\alpha_j}\frac{\alpha_{\max}}{\alpha_{\min}}}$. Moreover, based on (37) and after some algebraic manipulation, we obtain the expression of ξ_j.

G. Proof of Theorem 4

When $\beta\to\infty$ and $\alpha_1=\alpha_2=\alpha$, based on (37) and (38) and after some algebraic manipulation, we have

$$\Pr\left(\mathrm{SIR}_{j,0}>\beta\right)=\sum_{n=0}^{M_j-1}\frac{1}{n!}\sum_{n_1+n_2+n_3=n}\binom{n}{n_1,n_2,n_3}\sum_{(m_a)_{a=1}^{n_1}\in\mathcal{M}_{n_1}}\sum_{(p_a)_{a=1}^{n_2}\in\mathcal{M}_{n_2}}\sum_{(q_a)_{a=1}^{n_3}\in\mathcal{M}_{n_3}}\frac{n_1!}{\prod_{a=1}^{n_1}m_a!}$$

$$\times \beta^{-\sum_{a=1}^{n_1} m_a+\frac{2}{\alpha}\sum_{a=1}^{n_2} p_a+\frac{2}{\alpha}\sum_{a=1}^{n_3} q_a} \prod_{a=1}^{n_1}\left(\frac{\frac{2}{\alpha}\pi}{1+\frac{2}{\alpha}} p_{\bar{c}}(U,T_1,T_2)\lambda_1\left(\frac{P_1}{P_j}\right)^{\frac{2}{\alpha}}\left(T_j^{1+\frac{2}{\alpha}}-1\right)\right)^{m_a}$$
$$\times \frac{n_2!}{\prod_{a=1}^{n_2} p_a!}\prod_{a=1}^{n_2}\left(\frac{2\pi}{\alpha}\lambda_1\left(\frac{P_1}{P_j}\right)\mathrm{B}\left(1+\frac{2}{\alpha},a-\frac{2}{\alpha}\right)\right)^{p_a}\frac{n_3!}{\prod_{a=1}^{n_3} q_a!}\frac{\pi\lambda_j}{\mathcal{A}_j}$$
$$\times \prod_{a=1}^{n_3}\left(\frac{2\pi}{\alpha}\lambda_2\left(\frac{P_2}{P_j}\right)^{\frac{2}{\alpha}}\mathrm{B}\left(1+\frac{2}{\alpha},a-\frac{2}{\alpha}\right)\right)^{q_a}\Gamma\left(\sum_{a=1}^{n_1} m_a+\sum_{a=1}^{n_2} p_a+\sum_{a=1}^{n_3} q_a+1\right)$$
$$\times \frac{\beta^{-\frac{2}{\alpha}\left(\sum_{a=1}^{n_1} m_a+\sum_{a=1}^{n_2} p_a+\sum_{a=1}^{n_3} q_a+1\right)}}{\frac{2\pi}{\alpha}\mathrm{B}\left(\frac{2}{\alpha},1-\frac{2}{\alpha}\left(\lambda_1\left(\frac{P_1}{P_j}\right)^{\frac{2}{\alpha}}+\lambda_2\left(\frac{P_2}{P_j}\right)^{\frac{2}{\alpha}}\right)\right)^{\sum_{a=1}^{n_1} m_a+\sum_{a=1}^{n_2} p_a+\sum_{a=1}^{n_3} q_a+1}}. \quad (46)$$

From (46), we see that the order is $\beta^{-\left(1+\frac{2}{\alpha}\right)\sum_{a=1}^{n_1} m_a-\frac{2}{\alpha}}$, which can be maximised when $n_1 = 0$. Hence, the order is $\beta^{-\frac{2}{\alpha}}$. Moreover, after some algebraic manipulation, we can obtain the expression of the coefficient.

H. Proof of Lemma 4

We solve the optimization problem for $\alpha_1 = \alpha_2$. When $\alpha_1 \neq \alpha_2$, the optimization problem can be solved in a similar way and is omitted due to page limit. First, we rewrite $c_1(U,T_1,T_2)$ in (25) as $c_1(U,T_1,T_2) = \frac{\pi\lambda_1}{\mathcal{A}_1}\sum_{u=0}^{U}\Pr(u_{\mathrm{IN},0}=u)f(u)$, where $f(u)$ denotes the expression after $\Pr(u_{\mathrm{IN},0}=u)$ in (25). It can be easily verified that $f(u)$ is a decreasing function of u. By *Lemma 2*, we have $c_1(U,T_1,T_2) = \frac{\pi\lambda_1}{\mathcal{A}_1}\left(\sum_{u=0}^{U}\Pr(K_0=u)f(u)+\sum_{k=U+1}^{\infty}\Pr(K_0=k)f(U)\right)$. Thus, we have $c_1(U+1,T_1,T_2)-c_1(U,T_1,T_2) = \frac{\pi\lambda_1}{\mathcal{A}_1}(f(U+1)-f(U))\sum_{k=U+1}^{\infty}\Pr(K_0=k) < 0$. Therefore, we can show $U^*(\beta,T_1,T_2)=0$.

REFERENCES

[1] D. Lopez-Perez, I. Guvenc, G. de la Roche, M. Kountouris, T. Quek, and J. Zhang, "Enhanced intercell interference coordination challenges in heterogeneous networks," *Wireless Communications, IEEE*, vol. 18, no. 3, pp. 22–30, June 2011.

[2] A. Ghosh, N. Mangalvedhe, R. Ratasuk, B. Mondal, M. Cudak, E. Visotsky, T. Thomas, J. Andrews, P. Xia, H. Jo, H. Dhillon, and T. Novlan, "Heterogeneous cellular networks: From theory to practice," *Communications Magazine, IEEE*, vol. 50, no. 6, pp. 54–64, June 2012.

[3] D. Lee, H. Seo, B. Clerckx, E. Hardouin, D. Mazzarese, S. Nagata, and K. Sayana, "Coordinated multipoint transmission and reception in lte-advanced: deployment scenarios and operational challenges," *Communications Magazine, IEEE*, vol. 50, no. 2, pp. 148–155, February 2012.

[4] G. Nigam, P. Minero, and M. Haenggi, "Coordinated multipoint joint transmission in heterogeneous networks," *IEEE Trans. Commun.*, vol. 62, pp. 4134–4146, Nov. 2014.

[5] W. Nie, F. C. Zheng, X. Wang, S. Jin, and W. Zhang, "Energy efficiency of cross-tier base station cooperation in heterogeneous cellular networks," *submitted to IEEE Trans. Wireless Commun.*, 2014.

[6] A. Sakr and E. Hossain, "Location-aware cross-tier coordinated multipoint transmission in two-tier cellular networks," *Wireless Communications, IEEE Transactions on*, vol. 13, no. 11, pp. 6311–6325, Nov 2014.

[7] J. G. Andrews, F. Baccelli, and R. K. Ganti, "A tractable approach to coverage and rate in cellular networks," *IEEE Trans. Commun.*, vol. 59, no. 11, pp. 3122–3134, Nov. 2011.

[8] H. Dhillon, R. Ganti, F. Baccelli, and J. Andrews, "Modeling and analysis of k-tier downlink heterogeneous cellular networks," *Selected Areas in Communications, IEEE Journal on*, vol. 30, no. 3, pp. 550–560, April 2012.

[9] S. Singh and J. G. Andrews, "Joint resource partitioning and offloading in heterogeneous cellular networks," *IEEE Trans. Wireless Commun.*, vol. 13, no. 2, pp. 888–901, Feb. 2014.

[10] A. Adhikary, H. S. Dhillon, and G. Caire, "Massive-MIMO meets HetNet: Interference coordination through spatial blanking," *submitted to IEEE J. Select. Areas Commun.*, Jul. 2014.

[11] K. Hosseini, J. Hoydis, S. t. Brink, and M. Debbah, "Massive MIMO and small cells: How to densify heterogeneous networks," in *Proc. of IEEE Int. Conf. on Commun. (ICC)*, Budapest, Jun. 2013, pp. 5442–5447.

[12] M. Kountouris and N. Pappas, "HetNets and massive MIMO: Modeling, potential gains, and performance analysis," in *Proc. of IEEE-APS Topical Conference on APWC*, Torino, Italy, Sep. 2013, pp. 1319–1322.

[13] P. Xia, C. H. Liu, and J. G. Andrews, "Downlink coordinated multi-point with overhead modeling in heterogeneous cellular networks," *IEEE Trans. Wireless Commun.*, vol. 12, no. 8, pp. 4025–4037, Aug. 2013.

[14] Y. Wu, Y. Cui, and B. Clerckx, "Analysis and optimization of inter-tier interference coordination in downlink multi-antenna hetnets with offloading," *Wireless Communications, IEEE Transactions on*, vol. 14, no. 12, Dec 2015.

[15] K. Huang and J. G. Andrews, "An analytical framework for multicell cooperation via stochastic geometry and large deviations," *IEEE Trans. Inf. Theory*, vol. 59, no. 4, pp. 2501–2516, Apr. 2013.

[16] C. Li, J. Zhang, M. Haenggi, and K. Letaief, "User-centric intercell interference nulling for downlink small cell networks," *Communications, IEEE Transactions on*, vol. 63, no. 4, pp. 1419–1431, April 2015.

[17] S. Akoum and R. W. Heath Jr., "Interference coordination: random clustering and adaptive limited feedback," *IEEE Trans. Signal Process.*, vol. 61, no. 7, pp. 1822–1834, Apr. 2013.

[18] Y. Cui, Q. Huang, and V. Lau, "Queue-aware dynamic clustering and power allocation for network mimo systems via distributed stochastic learning," *Signal Processing, IEEE Transactions on*, vol. 59, no. 3, pp. 1229–1238, March 2011.

[19] R. Tanbourgi, S. Singh, J. G. Andrews, and F. K. Jondral, "A tractable model for noncoherent joint-transmission base station cooperation," *IEEE Trans. Wireless Commun.*, vol. 13, pp. 4959–4973, Sep. 2014.

[20] A. Hunter, J. Andrews, and S. Weber, "Transmission capacity of ad hoc networks with spatial diversity," *Wireless Communications, IEEE Transactions on*, vol. 7, no. 12, pp. 5058–5071, December 2008.

[21] T. Bai and R. W. Heath Jr., "Asymptotic coverage probability and rate in massive MIMO networks," 2013. [Online]. Available: http://arxiv.org/abs/1305.2233

[22] X. Zhang and M. Haenggi, "A stochastic geometry analysis of inter-cell interference coordination and intra-cell diversity," *IEEE Trans. Wireless Commun.*, vol. 13, pp. 6655–6669, Dec. 2014.

[23] M. Haenggi, "The mean interference-to-signal ratio and its key role in cellular and amorphous networks," *IEEE Wireless Commun. Lett.*, vol. 3, pp. 597–600, Dec. 2014.

[24] M. Haenggi and R. K. Ganti, "Interference in large wireless networks," *Foundations and Trends in Networking*, vol. 3, no. 2, pp. 127–248, 2009.

[25] W. P. Johnson, "The curious history of Faa di Bruno's formula," *The American Mathematical Monthly*, vol. 109, no. 3, pp. 217–234, Mar. 2002.